DOI: 10.1002/asia.200700295

Reversible Double-Helix–Random-Coil Transition Process of Bis{hexa(ethynylhelicene)}s

Hiroki Sugiura, Ryo Amemiya, and Masahiko Yamaguchi *[a]

Dedicated to Professor Teruaki Mukaiyama on the occasion of his 80th birthday

Abstract: Two compounds with two hexa(ethynylhelicene) parts connected by a flexible haxadecamethylene and a rigid butadiyne linker were synthesized. The ^{1}H NMR spectroscopic and CD analyses and vapor-pressure osmometry (VPO) of these two compounds revealed intramolecular double-helix formation. Upon heating a 5-μM solution in toluene, the double-helix structure unfolded to form a random coil, and on cooling it folded again into a double helix. The thermodynamic stabilities of both structures were dependent on temperature, and the structural change in both compounds is due to the large enthalpies and entropies under equilibrium. The rate constants of their unfolding were obtained by assuming a pseudo-first-order reaction; the compound with a rigid linker unfolded slower than that with a flexible linker. The former has a larger activation energy, and its double-helix and random-coil conformers were separated by chromatography. The rate of folding was also faster for the flexible-linker compound with larger activation energy. The rate constants for the folding of both compounds slightly decreased with increasing temperature, which was ascribed to the presence of exothermic pre-equilibrium and rate-determining steps. The folding was markedly accelerated with increasing random-coil concentration, which suggests the involvement of self-catalysis. A mechanism of folding was proposed. The involvement of different mechanisms of folding and unfolding was suggested by the kinetic studies, and it was confirmed by the presence of hysteresis in the melting profiles. The difference in linker structure also affected the thermal-switching profiles of the double-helix–random-coil structural changes.

Keywords: activation energy · helical structures · molecular switching · self-catalysis · structural transitions

Introduction

Molecular switching, which is a reversible structural change in response to changes in the environment, has attracted much attention.[1] The construction of synthetic switching compounds and the understanding of their properties are interesting subjects, the realization of which may lead to the development of switching systems that can be utilized in the biological and materials sciences.

Reversible structural changes in principle can be understood with a two-state model (Figure 1). In response to changes in the environment such as temperature, light, substrate concentration, the presence or absence of chemical substances, and chemical reactions, a molecule reversibly changes its thermodynamic stability between two states, X and Y, and changes its structure from X to Y or vice versa. A change in molecular ratio at equilibrium between the states X and Y, which is dependent on the energy difference between the two, is then detected by physical methods such as spectroscopy. As well as thermodynamic aspects, the chemical kinetics of the structural changes from X to Y and vice versa are also important, which are again affected by the environment. In kinetic studies, intermediates and transition-state structures and their energies are examined in relation to how a molecule responds to changes in the environment. To utilize reversible structural changes for molecular switching, both thermodynamic and kinetic properties need to be understood. This is an interesting subject of

[a] Dr. H. Sugiura, Dr. R. Amemiya, Prof. Dr. M. Yamaguchi
Department of Organic Chemistry
Graduate School of Pharmaceutical Sciences
Tohoku University
Aoba 6–3, Sendai 980-8578 (Japan)
Fax: (+81) 22-795-6811
E-mail: yama@mail.pharm.tohoku.ac.jp

Supporting information for this article is available on the WWW under http://www.chemasianj.org or from the author.

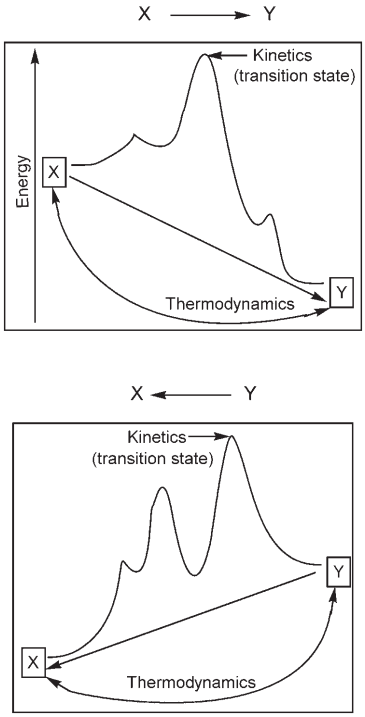

Figure 1. Schematic representation of reaction energy for reversible structural change between X and Y.

study on rather complex chemical-reaction systems. Although several synthetic switching molecules have been developed, the majority of studies have examined only the relationship between the changes in the environment and the differences between two structures.[1] Analyses of structural-change processes, particularly kinetic studies, are lacking.

The double-helix structure is an interesting molecular architecture formed with two linear molecules, and contains three-dimensional structural variations in terms of diameter, length, pitch, and chirality, among others, besides the one-dimensional arrangement of atoms.[2–9] The structure is formed by several noncovalent bond interactions such as hydrogen bonds, electrostatic interactions, van der Waals interactions, charge-transfer interactions, π–π interactions, and CH–π interactions, both in the intramolecular and intermolecular modes. This is in contrast to the single-helix structure, whose formation depends only on intramolecular interactions. The diversity of the structural features of a double helix makes its structural switching extremely interesting. DNA and RNA offer excellent examples of structural switching between a double helix and a random coil, and the kinetics of their structural changes have been examined to some detail.[10,11] In contrast, little is known about the kinetics of synthetic double-helix compounds.[12–15]

During our studies on the synthesis and properties of optically active helicene derivatives, hepta(ethynylhelicene) **1** was found to form a helix dimer, most likely a double helix, in organic solvents.[16] Whereas helical **1** irreversibly changes its structure to a random coil (unfolding) at low concentrations (5 μM), at high concentrations (1 mM), **1** reversibly changes its structure between the double helix and the random coil upon heating and cooling (unfolding and folding).[17] The ratio of the double helix to the random coil changes considerably depending on temperature, concentration, and solvent, which indicates the sensitivity of the thermochemical properties of the two structures. Another notable feature of compound **1** is the diversity in its rate of unfolding, and the rate constant varies over seven orders of magnitude depending on the solvent. Thus, it was considered to be an attractive system on which to conduct kinetic studies of the unfolding and folding of a double helix. To compare and understand the process of structural changes in **1**, we selected, in this study, compounds **2** and **3** containing two parts of the hexa(ethynylhelicene) moiety, which are linked by a flexible 3.0-nm-long hexadecamethylene linker and a rigid 3.0-nm-long butadiyne linker, respectively.[18] Compounds **2** and **3** were expected to form aggregate properties different from those of **1**. Such double-helix–random-coil transitions of linked compounds were examined with DNA[19,20] or RNA[21] derivatives. Depending on the structure of the linker moiety, the double-helix structure exhibits different thermal stabilities as shown by its melting profiles. We therefore considered it interesting to study the thermodynamics and kinetics of double-helix–random-coil transitions by using synthetic compounds that form linked double helices.

It was found that both **2** and **3** form similar intramolecular double-helix structures with similar thermodynamic properties. The double-helix–random-coil transitions of **2** and **3**, however, are dependent on the structure of the linker. The unfolding of **3** involves a higher activation energy than that of **2**, and the double-helix and random-coil conformers of **3** can be separated by chromatography. The folding of **2** and **3** involves a complex mechanism, which is not observed in the intermolecular folding of **1**. Separate

Abstract in Japanese:

ヘキサエチニルヘリセンを柔軟なヘキサデカメチレンリンカーまたは剛直なブタジインリンカーで連結したビス（ヘキサエチニルヘリセン）**2** および **3** を合成した。いずれの化合物も分子内二重ラセン構造を形成し、加熱と冷却によって分子内二重ラセン - ランダムコイル間で可逆的に構造変化した。**2** および **3** の二重ラセン - ランダムコイル構造間のエンタルピーとエントロピー変化は大きく、これが構造の温度変化依存性の原因である。リンカーの構造は二重ラセンの安定性にあまり影響しない。二重ラセンの解離反応の速度論的解析では、**2** は **3** よりも解離が速く、より小さな活性化エネルギーをもつ。会合反応ではいずれの化合物も温度の上昇に伴って反応速度が低下し、見かけ上、負の活性化エネルギーを与えた。**2** および **3** の会合反応は濃度依存性を示し、自己触媒反応であることも見出した。従って、**2** と **3** の会合と解離は異なる経路で進行することになり、融解曲線においてヒステリシスが観測された。二重ラセン - ランダムコイル構造間のスイッチングはリンカーの構造に強く依存した。**2** のスイッチングは 1 μM (55 °C/10 °C) で進行したが、**3** ではより高温と高濃度 (0.25 mM, 75 °C/10 °C) で行う必要があった。リンカーの構造によって解離反応と会合反応の遷移状態のエネルギーおよび構造が制御できることを示した。

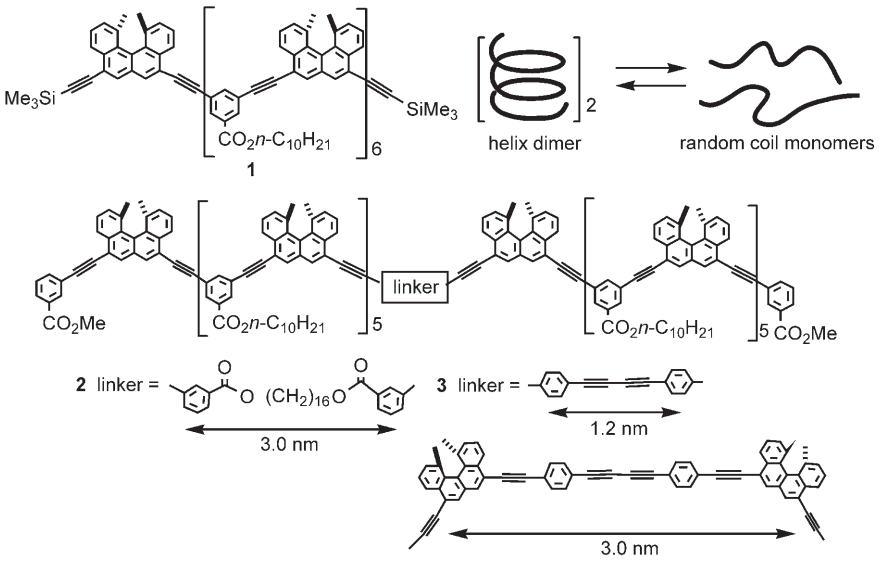

studies of unfolding and folding provide information that can be used to develop a molecular-switching system.

Results and Discussion

Synthesis

Derivatives **2** and **3** were synthesized from ethynylhelicene (*M*)-**4**[22] via hexa(ethynylhelicene) **19** by repeated Sonogashira coupling and deprotection (Scheme 1). A one-directional method was employed in this study because the two terminal parts of the oligomer should be differentiated. Compound (*M*)-**4** was coupled to 3-iodobenzoate **5** to obtain (*M*)-**6** in 96% yield. The treatment of (*M*)-**6** with Bu_4NF produced desilylated (*M*)-**7**, which was coupled to building block (*M*)-**8**[22] to obtain di(ethynylhelicene) **9**. Similar desilylation followed by Sonogashira coupling to (*M*)-**8** produced the ethynylhelicenes, from tri(ethynylhelicene) **10** to hepta(ethynylhelicene) **14**, in high yields.

The CD spectra of **13** and **14** with six or more helicenes in $CHCl_3$ at 5 μM exhibited a large Cotton effect in the regions 280–350 and 350–400 nm by the formation of chiral aggregation structures, which were previously assigned to the helix dimer or double-helix structure for **1** (Figure 2a),[16] whereas oligomers **9**–**12** with five or fewer helicenes formed random-coil structures (Figure 2b). On the basis of the confirmation of the effect of the chain length, we decided to prepare dimers from the hexamer **19**. Finally, the deprotected hexa(ethynylhelicene) **19** was coupled to diiodo linker **20** or **21** to yield the desired product **2** (53%) or **3** (45%), respectively (Scheme 1).

Folded Structure

The CD spectra of **2** (1 μM) in $CHCl_3$ 5 min after dissolution exhibited a large Cotton effect similar to those of **1**, **13**, and **14** in the regions 280–350 and 350–400 nm (Figure 3). When the solution was allowed to stand at 25°C, a slight attenuation of the Cotton effect was observed after 5 h. Helical **1** (5 μM) unfolded to form a random-coil structure 12 h after dissolution at 25°C.[16] The lower tendency of **2** to unfold relative to **1** may be due to the intramolecular helical aggregation of **2**. At 55°C, the unfolding of **2** occurred rapidly, and a random-coil structure was formed after 30 min.

The ^1H NMR spectra of **2** (1 mM) in $CDCl_3$ taken 30 min after dissolution were broadened in the aromatic region at 25°C and exhibited absorptions of aromatic protons up to $\delta =$ 5.2 ppm (Figure 4a). The spectra are similar to those of helical **1**.[16] When the solution was heated at 60°C for 24 h, the

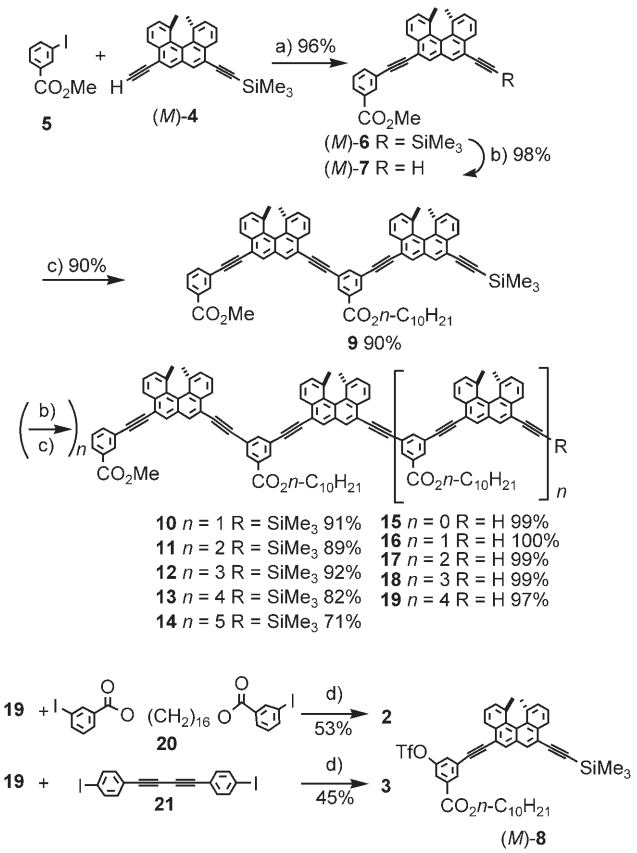

Scheme 1. Synthesis of **2** and **3**. Conditions: a) $[Pd(dba)_3]\cdot CHCl_3$, CuI, Mes_3P, Bu_4NI, NEt_3, DMF, 45°C, 1 h; b) Bu_4NF, THF, 0°C, 10 min; c) (*M*)-**8**, $[Pd(dba)_3]\cdot CHCl_3$, CuI, Mes_3P, Ph_3P, Bu_4NI, NEt_3, DMF/toluene or THF, 45°C, 1 h; d) $[Pd(dba)_3]\cdot CHCl_3$, CuI, Mes_3P, Bu_4NI, NEt_3, DMF/THF, 45°C, 2 h. dba = dibenzylideneacetone, DMF = *N*,*N*-dimethylformamide, Mes = mesityl, Tf = trifluoromethanesulfonyl.

CHEMISTRY
AN ASIAN JOURNAL

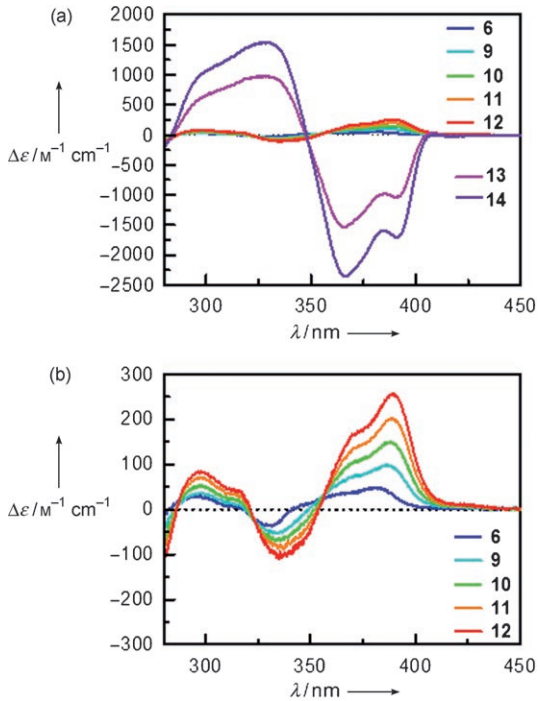

Figure 2. a) CD spectra of **6**, **9**, **10**, **11**, **12**, **13**, and **14** (5 μM, $CHCl_3$, 25 °C). b) CD spectra of **6**, **9**, **10**, **11**, and **12** (5 μM, $CHCl_3$, 25 °C). The spectra were obtained 5 min after dissolution.

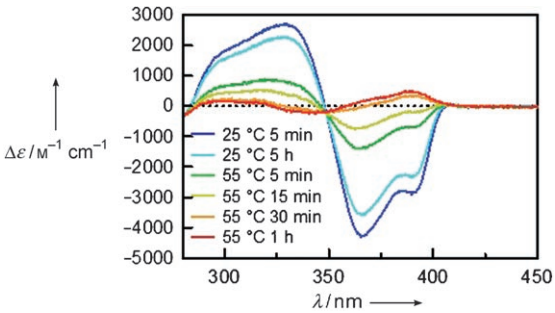

Figure 3. CD spectra of **2** (1 μM, $CHCl_3$) obtained at each time and temperature point studied after dissolution.

signal intensity of the random-coil conformer increased (Figure 4b). The helical structure of **2** completely unfolded to form a random coil after heating at 100 °C for 1 h in [D_8]toluene (Figure 4c).

Vapor-pressure osmometry (VPO) was performed. The CD spectra of **2** (0.5 mM) obtained 5 min and 6 h after dissolution confirmed that the helical structure of **2** was maintained (Figure 5a). The molecular weight of **2** was concentration-independent between 1 and 10 mM, which corresponds to that of the monomer (Figure 5b). These experiments indicate that **2** formed an intramolecular helix dimer or double helix.

The experiments described later provided the equilibrium constant K_{eq} and the Gibbs free-energy ΔG values of the

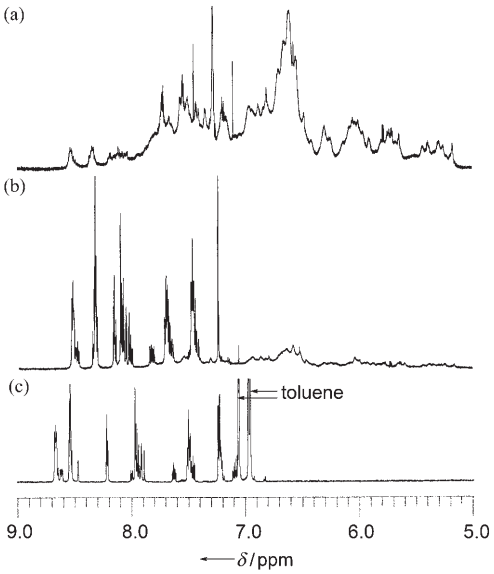

Figure 4. ^{1}H NMR (600 MHz, 1 mM) spectra of **2**. a) Observed at 25 °C, 30 min after dissolution in $CDCl_3$. b) Observed at 60 °C after heating at 60 °C for 24 h ($CDCl_3$). c) Observed at 100 °C after heating at 100 °C for 1 h in [D_8]toluene.

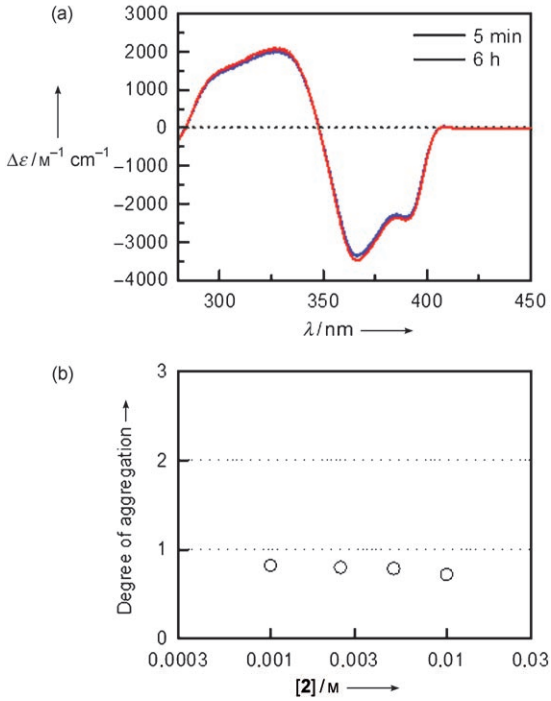

Figure 5. a) CD spectra of **2** (0.5 mM, 35 °C) 5 min and 6 h after dissolution in $CHCl_3$. b) Degree of aggregation of **2** determined by VPO (35 °C) at various concentrations after dissolution in $CHCl_3$. Degree of aggregation = (observed molecular weight)/(theoretical molecular weight of monomeric **2**).

double helix and random coil at equilibrium for **2**, from which $\Delta H = (+194 \pm 19)$ kJ mol^{-1} and $\Delta S = (+0.61 \pm 0.06)$ kJ K^{-1} mol^{-1} were obtained.[23] The large positive entropy is the origin of the substantial temperature dependence

of the equilibrium, which resulted in a sharp structural change. It was previously observed that compound **1** irreversibly unfolded at 5 μM, and folding occured only at 1 mM.[17] A similar experiment of the unfolding of **1** (1 mM) in toluene provided thermodynamic data at equilibrium: $\Delta H = (+98 \pm 18)$ kJ mol^{-1}, $\Delta S = (+0.33 \pm 0.06)$ kJ K^{-1} mol^{-1}.[23] The larger ΔH of **2** over **1** indicates that the intramolecular helical structure of **2** is thermodynamically more stable than the intermolecular helix dimer of **1**.

Next, compound **3**, which has a rigid butadiyne linker, was examined. The CD spectra of **3** (1 μM) recorded at 25 °C 5 min after dissolution in $CHCl_3$ exhibited a large Cotton effect in the regions 280–360 and 360–400 nm, which corresponds to the helical structure (Figure 6). The similarity of

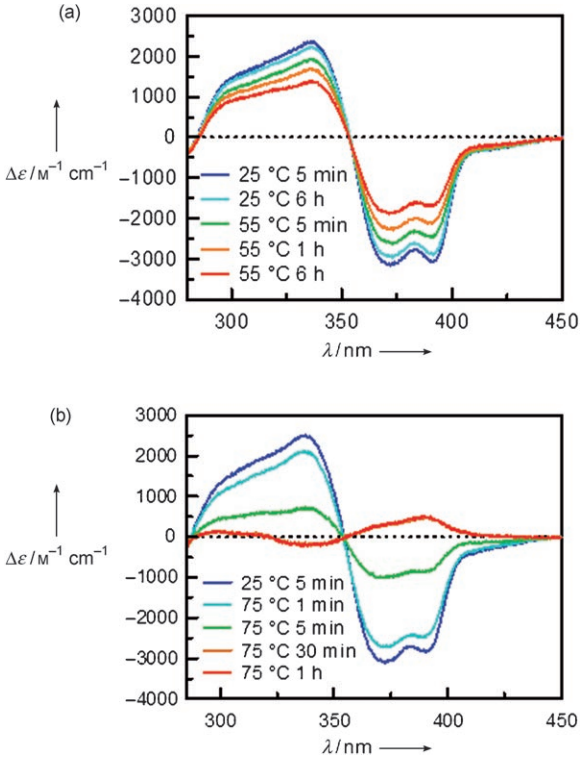

Figure 6. CD spectra (1 μM) of **3** obtained at each time and temperature point after dissolution in a) $CHCl_3$ and b) toluene.

the CD spectra of helical **1**, **2**, and **3** indicate similar structures despite the considerable difference in the features of the linker moiety. Although helical **2** unfolded to form a random-coil structure after heating at 55 °C for 30 min (Figure 3), the unfolding of **3** in $CHCl_3$ was not complete even after heating for 6 h at 55 °C. Random coil **3** was formed after heating at 75 °C for 30 min in toluene.

The helical-structure–random-coil transition of **3** was also observed by ^{1}H NMR spectroscopic analysis, and spectra similar to those of **2** were obtained.[23] Broad signals between $\delta = 5.0$ and 8.8 ppm were observed in the ^{1}H NMR ($CDCl_3$) spectrum of **3** at 25 °C, which sharpened when **3** was heated in [D_8]toluene at 100 °C for 1 h.

CD analysis and VPO revealed the monomeric nature of helical **3** in $CHCl_3$ between 1 and 10 mM, which is consistent with the formation of the intramolecular helix as in the case of **2** (Figure 7).

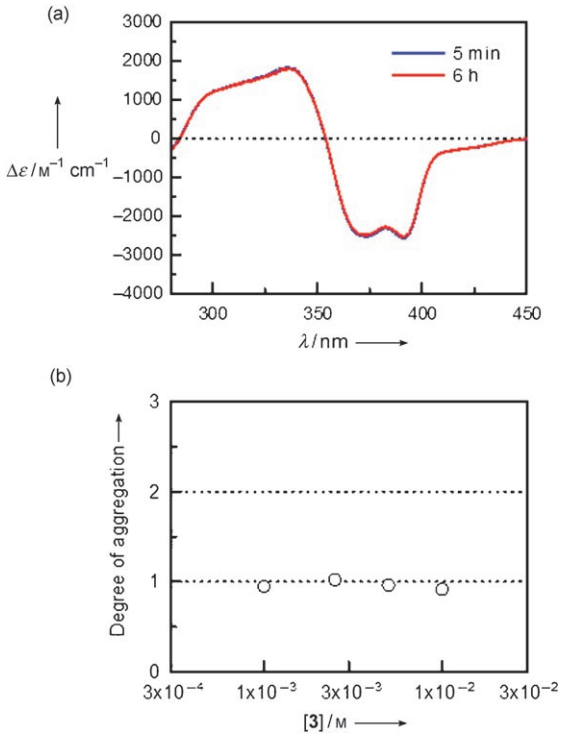

Figure 7. a) CD spectra of **3** (0.5 mM, 35 °C) 5 min and 6 h after dissolution in $CHCl_3$. b) Degree of aggregation of **3** (35 °C) determined by VPO at various concentrations after dissolution in $CHCl_3$.

A study of the unfolding of **3** (5 μM) in toluene provided thermodynamic data at equilibrium: $\Delta H = (+223 \pm 51)$ kJ mol^{-1}, $\Delta S = (+0.69 \pm 0.16)$ kJ K^{-1} mol^{-1}.[23] A comparison of the data with those of **2** revealed that the effect of the linker structure on the thermodynamic stability of **2** and **3** during their transition between the helical structure and the random coil is not large.

The intramolecular aggregate formation of **3** with thermodynamic properties and CD spectra similar to those of **2** may support the formation of the double-helix structures of **1**, **2**, and **3** rather than that of the helix-on-helix structure, in which two single helices interact with the bottom and top parts of each helix facing each other (Figure 8). Compounds **1** and **2** can form similar helix-on-helix structures. However, the helix-on-helix structure of **3** may be different from that of **2** because of the rigid linker moiety of **3**, and the thermodynamic properties of **3** may also be different from those of **2**. Figure 9 shows a proposed double-helix structure of **2**, which has a tubular structure with an outer diameter of 2 nm, an inner diameter of 0.85 nm, and a height of 2 nm.

CHEMISTRY
AN ASIAN JOURNAL

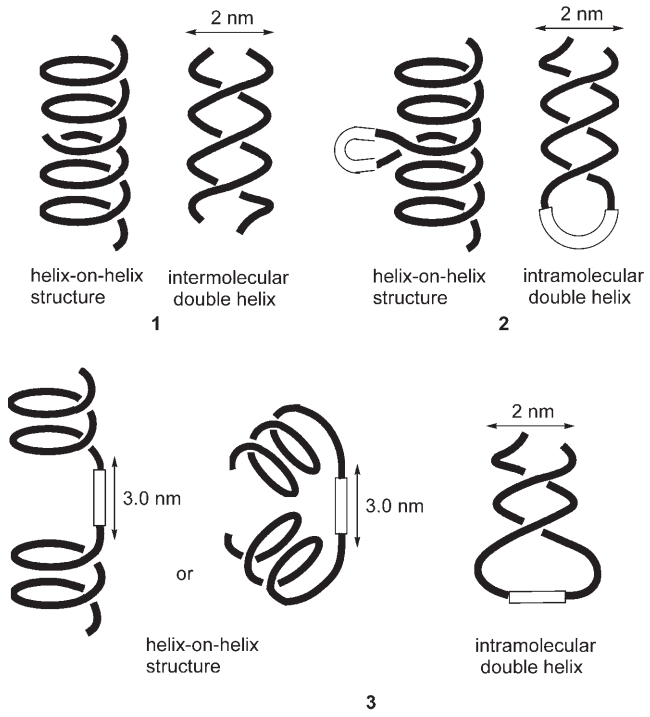

Figure 8. The double-helix structures of **1**, **2**, and **3**.

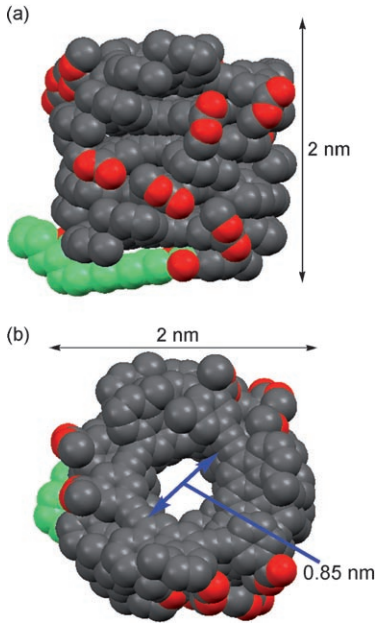

Figure 9. Proposed intramolecular double-helix structure of **2** obtained by MacroModel 8.6 (MM2* force field). The hexadecamethylene moiety is shown in green.

Unfolding Process

The double-helix–random-coil transitions of **2** and **3** were examined with CD spectroscopy in toluene. A 5-μM solution of helical **2** in toluene was prepared at 25 °C by dissolving **2** in toluene. The solution was rapidly heated to 75 °C, and the time dependence of Δε at 370 nm was measured (Figure 10).

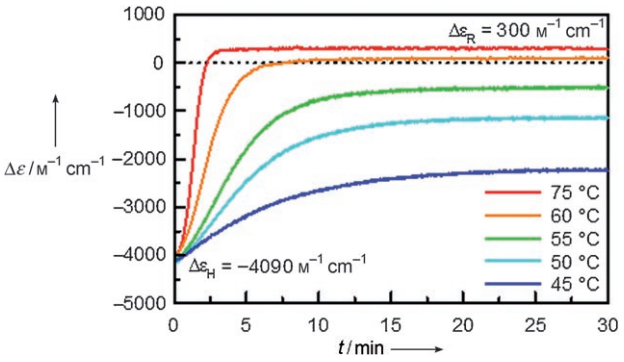

Figure 10. Time dependence of Δε at 370 nm for **2** (5 μM) in toluene at 75, 60, 55, 50, and 45 °C.

Upon heating, helical **2** with $\Delta\varepsilon_H = -4090\,M^{-1}cm^{-1}$ unfolded to form a random-coil structure with $\Delta\varepsilon_R = +300\,M^{-1}cm^{-1}$ within 5 min. To obtain the rate constant for unfolding at 60, 55, 50, and 45 °C at 5 μM, the Δε value at relatively low conversion after 1.5 min of heating was analyzed by assuming a pseudo-first-order reaction: $k = (4.6 \pm 0.1) \times 10^{-1}$ (60 °C), $(1.6 \pm 0.1) \times 10^{-1}$ (55 °C), $(1.0 \pm 0.1) \times 10^{-1}$ (50 °C), and $(4.7 \pm 0.1) \times 10^{-2}\,min^{-1}$ (45 °C). The rate constant $k = (1.9 \pm 1.6) \times 10^{-3}\,min^{-1}$ at 25 °C (5 μM) was estimated for **2** on the basis of the Arrhenius plot, which was found to be one order of magnitude smaller than that of **1** ($k = (1.9 \pm 0.1) \times 10^{-2}\,min^{-1}$) under the same conditions.[16] The rate was sensitive to temperature, and an activation energy $E_a = (133 \pm 17)\,kJ\,mol^{-1}$ was provided for unfolding, which is similar to that obtained for **1** ($E_a = (115 \pm 16)\,kJ\,mol^{-1}$).[23]

The rate constants in the unfolding of **3** were obtained in a manner similar to that for **2**.[23] The time dependence of Δε at 370 nm for **3** at 75, 70, 65, and 60 °C provided the rate constants for unfolding: $k = (4.3 \pm 0.1) \times 10^{-1}$ (75 °C), $(1.5 \pm 0.1) \times 10^{-1}$ (70 °C), $(6.1 \pm 0.3) \times 10^{-2}$ (65 °C), and $(3.5 \pm 0.2) \times 10^{-2}\,min^{-1}$ (60 °C) (Figure 11). From the Arrhenius plot, $k = (2.9 \pm 2.6) \times 10^{-5}\,min^{-1}$ at 25 °C and $E_a = (163 \pm 17)\,kJ\,mol^{-1}$ were obtained.[23] The unfolding rate of **3**, with $k = (1.9 \pm 1.6) \times 10^{-3}\,min^{-1}$ at 25 °C, is two orders of magnitude lower than that of **2**.

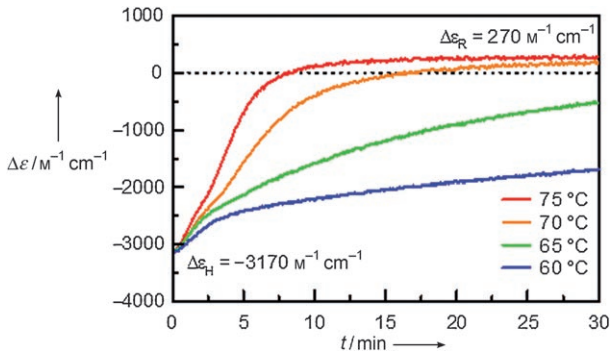

Figure 11. Time dependence of Δε at 370 nm for **3** (5 μM) in toluene at 75, 70, 65, and 60 °C.

The rate of monomolecular unfolding and the activation energy of **1**, **2**, and **3** decrease in the order **1** > **2** > **3** and **3** > **2** > **1**, respectively.

The activation energy $E_a = (163 \pm 17)\ \mathrm{kJ\,mol^{-1}}$ in the unfolding of **3** is considerably larger than that of **2** ($E_a = (133 \pm 17)\ \mathrm{kJ\,mol^{-1}}$), and the rigid linker increased the activation energy of unfolding. Accordingly, the double-helix and random-coil conformers of **3** were separable. Gel-permeation chromatography (GPC) of **3** in THF at ambient temperature showed two peaks (Figure 12). The CD spectra of each fraction were recorded without concentration, which showed that the first eluted fraction has the double-helix structure and the second, the random-coil structure.[23] The double-helix structure of the first eluted fraction slowly changed to the random-coil structure. In contrast, **2** eluted as a single fraction containing the random coil, as shown by GPC.[23]

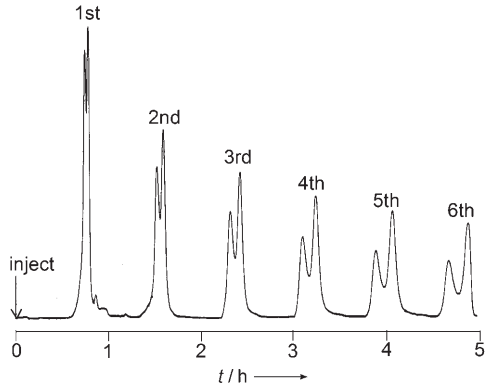

Figure 12. Recycle GPC chromatogram of **3** in THF at ambient temperature (JAIGEL 3H and 2H columns, flow rate 3.5 mL min^{-1}). A 10-mg sample of **3** was injected.

Folding Process

Next, the folding of **2** and **3** was examined. A 5-μM solution of **2** in toluene was heated at 75 °C for 30 min to complete unfolding, and the solution with the random coil was cooled to 20, 15, 10, or 5 °C. The folding was monitored by $\Delta\varepsilon$ at 370 nm (Figure 13). The folding started from $\Delta\varepsilon_R = +300\ \mathrm{M^{-1}cm^{-1}}$ and was completed within 120 min at these temperatures to yield $\Delta\varepsilon_H = -4090\ \mathrm{M^{-1}cm^{-1}}$. By using $\Delta\varepsilon$ at the initial stage of folding and assuming a pseudo-first-order reaction, the rate constants $k = (2.2 \pm 0.1) \times 10^{-1}$ (20 °C), $(2.7 \pm 0.1) \times 10^{-1}$ (15 °C), $(2.9 \pm 0.1) \times 10^{-1}$ (10 °C), and $(3.2 \pm 0.1) \times 10^{-1}\ \mathrm{min^{-1}}$ (5 °C) were obtained. The reaction was faster at lower temperatures, thus yielding the apparent negative activation energy $E_a = (-13 \pm 4)\ \mathrm{kJ\,mol^{-1}}$.[23] Such a phenomenon was previously observed in folding DNA and RNA[10,11] and was explained by the presence of an exothermic pre-equilibrium and a rate-determining step with a small activation energy.[24]

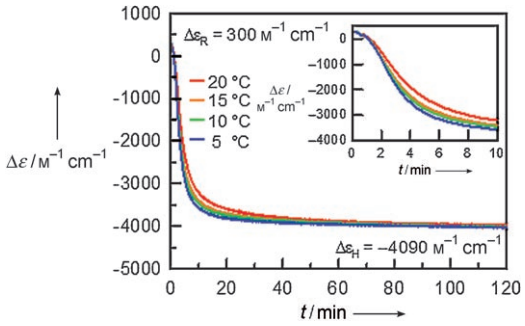

Figure 13. Time dependence of $\Delta\varepsilon$ at 370 nm for **2** (5 μM) in toluene at 20, 15, 10, and 5 °C after heating at 75 °C for 30 min. Inset: magnified graph.

The folding rates of **3** (5 μM) in toluene were also measured, and the rate constants were determined to be $k = (6.4 \pm 0.3) \times 10^{-3}$ at 20 °C, $(9.1 \pm 0.3) \times 10^{-3}$ at 15 °C, $(1.2 \pm 0.3) \times 10^{-2}$ at 10 °C, and $(1.7 \pm 0.4) \times 10^{-2}\ \mathrm{min^{-1}}$ at 5 °C (Figure 14).[23] As with **2**, the rate increased at lower temperatures, and the negative activation energy $E_a = (-43 \pm 2)\ \mathrm{kJ\,mol^{-1}}$ was obtained.[23] The folding rate constants of **3** are one order of magnitude smaller than those of **2** at the same temperatures. The kinetic analysis of **1** in the folding also showed a negative activation energy $E_a = (-44 \pm 3)\ \mathrm{kJ\,mol^{-1}}$,[23] and the folding process involved may be similar for **1**, **2**, and **3** in the rate-determining steps.

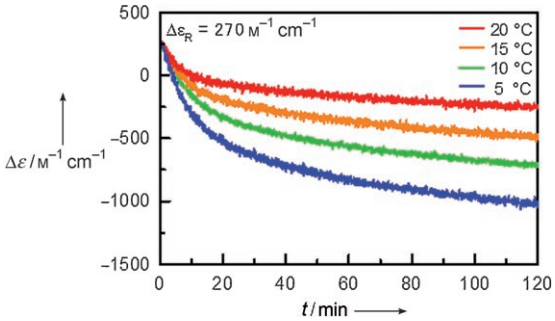

Figure 14. Time dependence of $\Delta\varepsilon$ at 370 nm for **3** (5 μM) in toluene at 20, 15, 10, and 5 °C after heating at 75 °C for 30 min.

A notable feature of the folding of **2** and **3** is its concentration dependence despite the apparent intramolecular first-order reaction. This is in contrast to the unfolding of **2** and **3**, which are concentration-independent.[23] The rate constants k of the folding of **2** changed more than tenfold from $(2.4 \pm 0.1) \times 10^{-2}$ (0.1 μM) to $(4.1 \pm 0.1) \times 10^{-1}\ \mathrm{min^{-1}}$ (7 μM), and plots of k against concentration show a linear relationship (Figure 15a). Similarly, the rate constants of the folding of **3** increased threefold with an increase in concentration from $(4.9 \pm 0.1) \times 10^{-3}$ (1 μM), to $(1.7 \pm 0.1) \times 10^{-2}\ \mathrm{min^{-1}}$ (7 μM) (Figure 15b).[23] These phenomena were attributed to self-catalysis, as reported for apparent first-order reactions such as the epimerization of chlorophyll[25] and the isomerization of aldose[26] or enol.[27]

CHEMISTRY
AN ASIAN JOURNAL

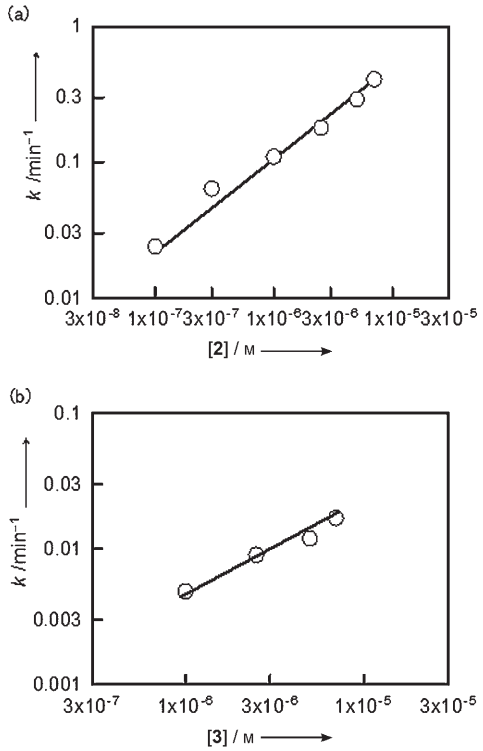

Figure 15. Plots of concentration versus rate constant k for the folding of a) **2** and b) **3** in toluene at 10 °C.

A model system is provided to explain the observations. It may be reasonably assumed that double-helix formation is initiated at the terminal helicene moiety rather than at the internal helicene moiety in the head-to-tail mode (Scheme 2a): The folding of **1A**, which is the random coil form of **1**, provides double helix **1C** via **1B**, and unfolds by the reverse process from **1C** to **1A**. If this assumption was true, the intramolecular folding of **2A**, the random coil form of **2**, to form double helix **2C** via intramolecular aggregate **2B** would be unlikely to occur, because the process requires the rearrangement of the conformer from the head-to-head mode to the head-to-tail mode (Scheme 2b). Thus, random coil **2A** should form intermolecular double helix **2E** via partial double helix **2D**, and then **2E** should fold to form intramolecular double helix **2C** via **2F** by extruding one of the **2A** forms. The unfolding from **2C** to **2A** may be a monomolecular dissociation reaction analogous to that from **1C** to **1A**. This explanation is consistent with the lack of hysteresis in the change of **1** (see below), because such self-catalysis cannot occur. The negative activation energy of folding of **2** may be explained by this mechanism: The folding from **2A** to **2D** occurs in the exothermic pre-equilibrium stage, and a rate-determining step with a small activation energy exists somewhere in the process between **2D** and **2C**.

The folding of **2** and **3** was suggested to involve self-catalysis (intermolecular reaction), whereas the unfolding involves a monomolecular reaction. The different properties of folding and unfolding suggest the involvement of different mechanisms, which was confirmed by a melting-profile study with UV/Vis spectroscopy (Figure 16). A 1-μM solution of **2** in toluene was heated from 17 to 75 °C at the rate of 1 °C min^{-1}, and the solution was then cooled to 17 °C at the same rate. The structural changes monitored by ε at 340 nm exhibited hysteresis (Figure 16b).

The melting profile of **3** (0.25 mM) determined from ε at 430 nm again exhibited hysteresis (Figure 17). As noted later, the reversible structural change of **3** required a higher concentration. In contrast to **2** and **3**, no hysteresis was observed in the analysis of **1** conducted at 1 mM (Figure 18), which is consistent with the mechanism described in Scheme 2.

Molecular Switching

Separate studies of the unfolding and folding of **2** and **3** provided information on the thermodynamic and kinetic properties of the structural changes. The information can be utilized for the development of a molecular-switching system, which should be constructed with the appropriate combinations of unfolding and folding.

It may be worthwhile to consider that the term "molecular switching" has a meaning somewhat different from that of "reversible structural change". As described above, the latter refers to the structural change in the system, which in principle is reversible, and the former emphasizes the practical aspects of the structural change. Molecular switching in this study is defined as follows: 1) The equilibrium shifts to the predominant formation of both the structures X and Y (Figure 1),

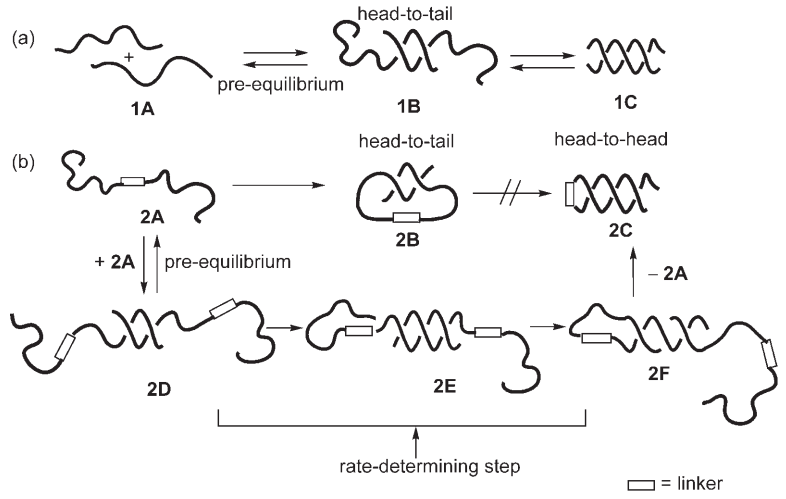

Scheme 2. Model system of double-helix formation.

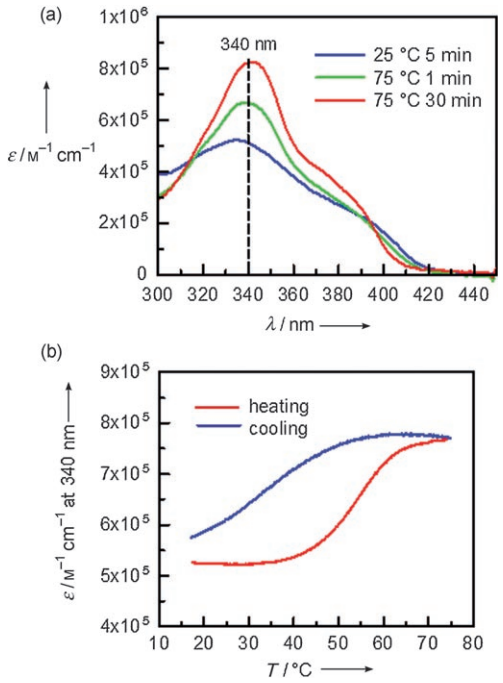

Figure 16. a) UV/Vis spectra of **2** (1 μM, toluene) obtained at each time and temperature point studied after dissolution. b) Melting profiles of **2** at 340 nm (toluene, 1 μM). The heating and cooling rates were both 1 °C min^{-1}.

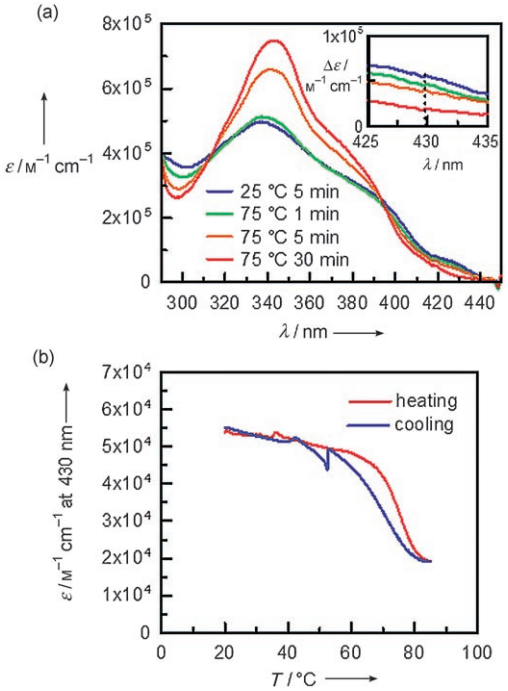

Figure 17. a) UV/Vis spectra of **3** (1 μM) obtained at each time and temperature point studied after dissolution in toluene. b) Melting profiles of **3** at 430 nm (0.25 mM, toluene). The heating and cooling rates were both 0.5 °C min^{-1}.

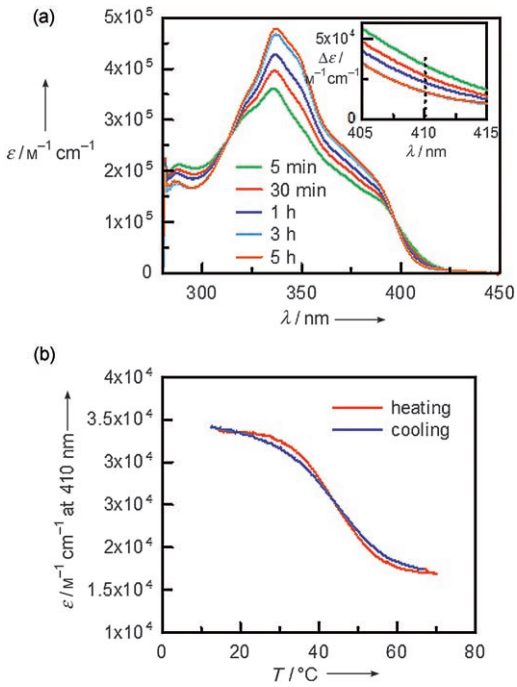

Figure 18. a) Time dependence of the UV/Vis spectra of **1** (5 μM) at 25 °C in toluene. Inset: magnification of the visible region. b) Melting profiles of **1** at 410 nm (toluene, 1 mM). The heating and cooling rates were both 1 °C min^{-1}.

so that the structural change is significant and can be readily detected; 2) the rate of structural change is sufficiently high for effective repetition; and 3) the process is highly reproducible. It may not be appropriate to call it "molecular switching" if a very slight structural change that is difficult to detect proceeds slowly for years. Thus, the conditions leading to molecular switching are restricted compared with those leading to reversible structural change.

On the basis of the thermodynamics and kinetics of unfolding and folding examined in this study, the conditions for the molecular switching of **2** and **3** in toluene have been clarified. Substantial differences in the rates of structural change between **2** and **3** indicate the critical role of linkers in molecular switching. The double-helix–random-coil switching of **2** can proceed at 1 μM at temperatures close to ambient: When a 1-μM solution of **2** in toluene was subjected to thermal cycles of heating at 55 °C and cooling at 10 °C every 30 min, **2** exhibited $\Delta\varepsilon$ cycles of $+20/-3270\,M^{-1}cm^{-1}$ (Figure 19). This is in contrast to the molecular switching of **1**, which requires 10^3 times higher concentrations of **1** (1 mM) to accelerate intermolecular folding.[16] The concentration dependence of the double-helix–random-coil switching profile of **2** is consistent with the different mechanisms underlying folding and unfolding. The slopes show that folding rate markedly decreases at lower concentrations (blue lines), but unfolding rate is not affected by concentration (red lines).

Although the folding and unfolding mechanisms of **3** are similar to those of **2**, the reaction rates of **3** are considerably lower than those of **2**. This becomes clear when the double-helix–random-coil switching of **3** (1 μM) was conducted with

CHEMISTRY
AN ASIAN JOURNAL

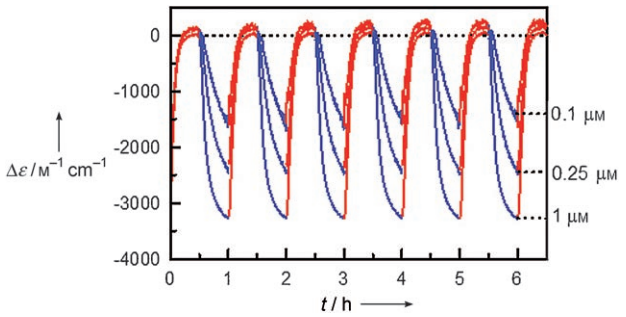

Figure 19. Concentration dependence of ($\Delta\varepsilon$ at 370 nm)–time profiles of **2** in toluene for repeated cycles of heating at 55 °C (red) and cooling at 10 °C (blue) every 30 min.

the same temperature cycles of 55/10 °C (Figure 20a). The $\Delta\varepsilon$ value of **3** is smaller and not highly reproducible compared with that of **2** (Figure 19). The switching of **3** required

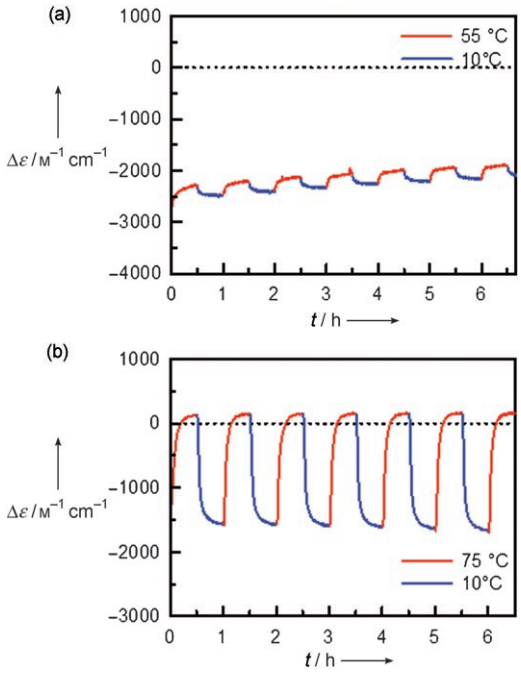

Figure 20. a) ($\Delta\varepsilon$ at 370 nm)–time profiles of **3** (1 μм) in toluene for repeated cycles of heating at 55 °C and cooling at 10 °C every 30 min. b) ($\Delta\varepsilon$ at 370 nm)–time profiles of **3** (0.25 мм) in toluene for repeating cycles of heating at 75 °C and cooling at 10 °C every 30 min.

a higher temperature and a higher concentration to accelerate both unfolding and folding and to shift the equilibrium: Switching can be conducted at 0.25 мм at 75/10 °C temperature cycles to provide reproducible $\Delta\varepsilon$ cycles of $+130/-1560\,м^{-1}cm^{-1}$ (Figure 20b). Thus, the change in the linker structure considerably affects the switching profiles, that is, the switching profiles can sensitively indicate the changes in the mechanisms of folding and unfolding.

Conclusions

Bis{hexa(ethynylhelicene)}s with a flexible hexadecamethylene linker **2** and a rigid butadiyne linker **3** were synthesized, both of which form an intramolecular double-helix structure. Thermodynamic and kinetic studies of their unfolding and folding were conducted separately. The thermodynamic parameters under the temperature-dependent equilibrium of **2** and **3** were similar, which indicate similar double-helix structures in the two compounds. The unfolding of the intramolecular double-helix structure to form the random-coil structure, which is a monomolecular reaction, was accelerated at higher temperature, and the activation energy for **3** is higher than that for **2**. Accordingly, the double-helix and random-coil conformers of **3** were separable. The mechanism of the folding is rather complex: The folding of **2** and **3** was accelerated at a lower temperature, which suggests the presence of pre-equilibrium and a rate-determining step; their folding rate was concentration-dependent, which suggests the involvement of self-catalysis. As the folding rate of **3** was lower than that of **2**, the molecular switching of **3** occurred only at concentrations and temperatures higher than those for **2**. It was shown that the structure of the linker has a strong effect on intramolecular double-helix–random-coil transition.

Experimental Section

Synthesis of bis{hexa(ethynylhelicene)s}

(*M*)-**6**: (*M*)-3-[1,12-Dimethyl-8-(trimethylsilylethynyl)benzo[*c*]phenanthren-5-ylethynyl]benzoic acid methyl ester: Under argon atmosphere, a mixture of **5** (116 mg, 0.443 mmol), tris(dibenzylideneacetone)dipalladium(0) chloroform adduct (11.5 mg, 0.0111 mmol), cuprous iodide (25.3 mg, 0.133 mmol), trimesitylphosphine (25.8 mg, 0.0664 mmol), tetrabutylammonium iodide (327 mg, 0.885 mmol), triethylamine (0.4 mL), and *N*,*N*-dimethylformamide (3 mL) was freeze-evacuated three times. A solution of (*M*)-**4** (167 mg, 0.443 mmol) in *N*,*N*-dimethylformamide (5 mL) was freeze-evacuated three times and added dropwise to the above solution. The mixture was stirred at room temperature for 1 h. The reaction was quenched by adding saturated aqueous ammonium chloride, and the organic materials were extracted with toluene. The organic layer was washed with brine and dried over magnesium sulfate. The solvents were evaporated under reduced pressure, and separation by recycling GPC gave (*M*)-**6** (217 mg, 0.425 mmol, 96 %). $[\alpha]_D^{23}=+507$ (*c* 1.00, $CHCl_3$); UV/Vis ($CHCl_3$, 5 μм): λ (ε) = 332 nm ($8.8\times10^4\,м^{-1}cm^{-1}$); CD ($CHCl_3$, 5 μм): λ ($\Delta\varepsilon$) 297 (31), 331 (−36), 380 nm ($49\,м^{-1}cm^{-1}$); IR (KBr): $\tilde{\nu}$ = 2207, 2145, 1725 cm^{-1}; ^{1}H NMR (600 MHz, $CDCl_3$): δ = 0.39 (s, 9H), 1.93 (s, 3H), 1.94 (s, 3H), 3.98 (s, 3H), 7.44 (d, *J* = 7.9 Hz, 1H), 7.46 (d, *J* = 7.9 Hz, 1H), 7.51 (dd, *J* = 7.9, 7.6 Hz, 1H), 7.66 (dd, *J* = 8.3, 7.9 Hz, 1H), 7.68 (t, *J* = 7.9 Hz, 1H), 7.87 (ddd, *J* = 7.6, 1.7, 1.0 Hz, 1H), 8.02 (s, 1H), 8.04 (s, 1H), 8.06 (ddd, *J* = 7.9, 1.7, 1.4 Hz, 1H), 8.37 (dd, *J* = 1.4, 1.0 Hz, 1H), 8.42 (d, *J* = 8.3 Hz, 1H), 8.50 ppm (d, *J* = 7.9 Hz, 1H); ^{13}C NMR (150 MHz, $CDCl_3$): δ = 0.1, 23.1, 23.1, 52.2, 88.6, 93.5, 100.0, 103.1, 119.8, 120.2, 123.5, 123.6, 123.7, 126.4, 126.8, 128.5, 129.0, 129.1, 129.3, 129.5, 129.8, 130.5, 130.8, 130.9, 130.9, 132.1, 132.2, 132.7, 135.7, 136.6, 136.7, 166.3 ppm; MS (EI): *m/z* (%) calcd for $C_{35}H_{30}O_2Si$: 510.2015 (100) $[M]^+$; found: 510.2036.

(*M*)-**7**: (*M*)-3-(8-Ethynyl-1,12-dimethylbenzo[*c*]phenanthren-5-ylethynyl)benzoic acid methyl ester: Typical procedure for desilylation: Tetrabutylammonium fluoride (1.0 м) in tetrahydrofuran (0.23 mL, 0.23 mmol) was added to a solution of (*M*)-**6** (67.5 mg, 0.132 mmol) in tetrahydrofu-

ran (2 mL) at 0 °C. After the mixture was stirred for 10 min at 0 °C, saturated aqueous ammonium chloride was added to it. The organic materials were extracted with ethyl acetate. The organic layer was washed with brine and dried over magnesium sulfate. The solvent was evaporated under reduced pressure; silica-gel chromatography (hexane/ethyl acetate = 10:1) gave (*M*)-**7** (57 mg, 0.130 mmol, 98 %). $[\alpha]_D^{22} = +500$ (*c* 1.00, $CHCl_3$); UV/Vis ($CHCl_3$, 5 μM): λ (ε) = 328 nm (8.0×10^4 M^{-1}cm^{-1}); CD ($CHCl_3$, 5 μM): λ ($\Delta\varepsilon$) = 294 (29), 328 (−39), 380 nm (44 M^{-1}cm^{-1}); IR (KBr): $\tilde{\nu}$ = 3281, 2208, 2096, 1721 cm^{-1}; ^{1}H NMR (600 MHz, $CDCl_3$): δ = 1.95 (s, 6H), 3.56 (s, 1H), 3.98 (s, 3H), 7.46 (d, *J* = 7.2 Hz, 1H), 7.47 (d, *J* = 7.6 Hz, 1H), 7.51 (dd, *J* = 7.9, 7.6 Hz, 1H), 7.66 (dd, *J* = 7.9, 7.2 Hz, 1H), 7.70 (dd, *J* = 8.2, 7.6 Hz, 1H), 7.87 (d, *J* = 7.6 Hz, 1H), 8.06 (s, 1H), 8.07 (s, 1H), 8.07 (1H, d, *J* = 7.9 Hz), 8.37 (s, 1H), 8.45 (d, *J* = 7.9 Hz, 1H), 8.51 ppm (d, *J* = 8.2 Hz, 1H); ^{13}C NMR (150 MHz, $CDCl_3$): δ = 23.2, 52.3, 81.8, 82.4, 88.6, 93.6, 119.3, 120.0, 123.5, 123.6, 123.8, 126.7, 126.9, 126.9, 128.6, 129.2, 129.4, 129.6, 130.4, 130.6, 130.9, 130.9, 130.9, 132.2, 132.3, 132.8, 135.8, 136.8, 136.9, 166.4 ppm; MS (EI): *m/z* (%) calcd for $C_{32}H_{22}O_2$: 438.1620 (100) $[M]^+$; found: 438.1604.

9: Typical procedure for the Sonogashira coupling reaction: Under argon atmosphere, a mixture of (*M*)-**8** (321 mg, 0.410 mmol), tris(dibenzylideneacetone)dipalladium(0) chloroform adduct (10.6 mg, 0.0102 mmol), cuprous iodide (23.4 mg, 0.123 mmol), trimesitylphosphine (23.9 mg, 0.0615 mmol), triphenylphosphine (16.1 mg, 0.0614 mmol), tetrabutylammonium iodide (303 mg, 0.820 mmol), triethylamine (0.5 mL), and *N*,*N*-dimethylformamide (5 mL) was freeze-evacuated three times. A solution of (*M*)-**7** (180 mg, 0.410 mmol) in *N*,*N*-dimethylformamide (5 mL) was freeze-evacuated three times, and was added dropwise to the above solution. The mixture was stirred for 1 h at 45 °C. The reaction was quenched by adding saturated aqueous ammonium chloride, and the organic materials were extracted with toluene. The organic layer was washed with brine and dried over magnesium sulfate. The solvents were evaporated under reduced pressure; separation by recycling GPC gave **9** (395 mg, 0.368 mmol, 90 %). M.p.: 218–220 °C (hexane–ethyl acetate); $[\alpha]_D^{23} = +566$ (*c* 1.00, $CHCl_3$); UV/Vis ($CHCl_3$, 5 μM): λ (ε) = 335 nm (1.5×10^5 M^{-1}cm^{-1}); CD ($CHCl_3$, 5 μM): λ ($\Delta\varepsilon$) = 298 (38), 332 (−53), 388 nm (98 M^{-1}cm^{-1}); IR (KBr): $\tilde{\nu}$ = 2206, 2145, 1724 cm^{-1}; ^{1}H NMR (600 MHz, $CDCl_3$): δ = 0.39 (s, 9H), 0.86 (t, *J* = 7.1 Hz, 3H), 1.24–1.37 (m, 10H), 1.41 (quin, *J* = 7.1 Hz, 2H), 1.51 (quin, *J* = 7.9 Hz, 2H), 1.86 (quin, *J* = 7.0 Hz, 2H), 1.94 (s, 3H), 1.95 (s, 3H), 1.98 (s, 6H), 3.98 (s, 3H), 4.43 (t, *J* = 6.7 Hz, 2H), 7.46 (d, *J* = 7.2 Hz, 1H), 7.48–7.51 (m, 3H), 7.52 (dd, *J* = 7.9, 7.6 Hz. 1H), 7.67 (dd, *J* = 7.9, 7.2 Hz, 1H), 7.70–7.75 (m, 3H), 7.89 (ddd, *J* = 7.6, 1.7, 1.0 Hz, 1H), 8.04 (s, 1H), 8.07 (ddd, *J* = 7.9, 1.7, 1.0 Hz, 1H), 8.09 (s, 1H), 8.11 (s, 1H), 8.14 (s, 1H), 8.20 (dd, *J* = 1.7, 1.4 Hz, 1H), 8.36 (dd, *J* = 1.7, 1.4 Hz, 2H), 8.39 (t, *J* = 1.7 Hz, 1H), 8.43 (d, *J* = 7.9 Hz, 1H), 8.52–8.56 ppm (m, 3H); ^{13}C NMR (150 MHz, $CDCl_3$): δ = 0.1, 14.1, 2.7, 23.1, 23.2, 23.2, 26.1, 28.7, 29.3, 29.5, 29.6, 31.9, 52.3, 65.8, 88.6, 89.3, 89.4, 92.9, 93.0, 93.7, 100.2, 103.1, 119.7, 119.8, 120.1, 120.3, 123.6, 123.6, 123.6, 123.7, 123.8, 124.3, 124.3, 126.7, 126.7, 126.9, 126.9, 127.0, 127.0, 128.6, 129.1, 129.2, 129.2, 129.3, 129.4, 129.6, 129.9, 130.6, 130.9, 131.0, 131.0, 131.1, 131.5, 132.1, 132.2, 132.2, 132.4, 132.4, 132.8, 135.8, 136.8, 136.9, 136.9, 138.3, 165.4, 166.4 ppm; MS (FAB, NBA (*m*-nitrobenzyl alcohol)): *m/z* calcd for $C_{76}H_{68}O_4Si$: 1072.4887 $[M]^+$; found: 1072.48464; elemental analysis: calcd (%) for $C_{76}H_{68}O_4Si$: C 85.04, H 6.39; found: C 84.96, H 6.39.

15: This compound (365 mg, 0.365 mmol, 99 %) was prepared from **9** (395 mg, 0.368 mmol). M.p.: 118–120 °C (hexane/ethyl acetate); $[\alpha]_D^{22} = +575$ (*c* 1.00, $CHCl_3$); UV/Vis ($CHCl_3$, 5 μM): λ (ε) = 333 nm (1.4×10^5 M^{-1}cm^{-1}); CD ($CHCl_3$, 5 μM): λ ($\Delta\varepsilon$) = 298 (38), 330 (−51), 388 nm (93 M^{-1}cm^{-1}); IR (KBr): $\tilde{\nu}$ = 3290, 2205, 2103, 1723 cm^{-1}; ^{1}H NMR (600 MHz, $CDCl_3$): δ = 0.86 (t, *J* = 7.0 Hz, 3H), 1.24–1.38 (m, 10H), 1.41 (quin, *J* = 6.9 Hz, 2H), 1.51 (quin, *J* = 7.7 Hz, 2H), 1.86 (quin, *J* = 7.1 Hz, 2H), 1.96 (s, 6H), 1.98 (s, 6H), 3.57 (s, 1H), 3.98 (s, 3H), 4.42 (t, *J* = 6.7 Hz, 2H), 7.47 (d, *J* = 7.1 Hz, 1H), 7.49–7.51 (m, 3H), 7.52 (dd, *J* = 7.9, 7.6 Hz, 1H), 7.67 (dd, *J* = 8.1, 7.1 Hz, 1H), 7.70–7.74 (m, 3H), 7.89 (dt, *J* = 7.6, 1.4 Hz, 1H), 8.07 (dt, *J* = 7.9, 1.4 Hz, 1H), 8.07 (s, 1H), 8.11 (s, 2H), 8.13 (s, 1H), 8.19 (dd, *J* = 1.7, 1.4 Hz, 1H), 8.36 (t, *J* = 1.7 Hz, 1H), 8.37 (dd, *J* = 1.7, 1.4 Hz, 1H), 8.39 (t, *J* = 1.4 Hz, 1H), 8.45 (d, *J* = 8.1 Hz, 1H), 8.52–8.56 ppm (m, 3H); ^{13}C NMR (150 MHz, $CDCl_3$): δ = 14.1, 22.7, 22.7, 23.2, 23.2, 26.0, 28.7, 29.3, 29.3, 29.5, 29.6, 31.9, 31.9, 52.3, 65.8, 81.8, 82.4, 88.6, 89.3, 89.3, 93.0, 93.7, 119.4, 119.8, 119.8, 120.1, 123.5, 123.6, 123.6, 123.6, 123.8, 124.3, 124.3, 126.7, 126.8, 126.9, 127.0, 127.0, 128.6, 129.2, 129.2, 129.3, 129.3, 129.4, 129.6, 129.8, 129.9, 130.4, 130.6, 130.8, 130.9, 131.0, 131.0, 131.1, 131.5, 132.2, 132.2, 132.4, 132.8, 135.8, 136.8, 136.9, 136.9, 138.3, 165.4, 166.4 ppm; MS (FAB, NBA): *m/z* calcd for $C_{73}H_{60}O_4$: 1000.4492 $[M]^+$; found: 1000.4547; elemental analysis: calcd (%) for $C_{73}H_{60}O_4$: C 87.57, H 6.04; found: C 87.47, H 6.09.

10: This compound (544 mg, 0.332 mmol, 91 %) was prepared from **15** (365 mg, 0.365 mmol) and (*M*)-**8** (286 mg, 0.365 mmol). M.p.: 204–205 °C (ethyl acetate); $[\alpha]_D^{23} = +562$ (*c* 1.00, $CHCl_3$); UV/Vis ($CHCl_3$, 5 μM): λ (ε) = 337 nm (2.3×10^5 M^{-1}cm^{-1}); CD ($CHCl_3$, 5 μM): λ ($\Delta\varepsilon$) = 298 (53), 333 (−69), 388 nm (150 M^{-1}cm^{-1}); IR (KBr): $\tilde{\nu}$ = 2206, 2147, 1723 cm^{-1}; ^{1}H NMR (600 MHz, $CDCl_3$): δ = 0.39 (s, 9H), 0.86 (t, *J* = 7.1 Hz, 6H), 1.24–1.38 (m, 20H), 1.38–1.44 (m, 4H), 1.48–1.53 (m, 4H), 1.83–1.89 (m, 4H), 1.94 (s, 3H), 1.95 (s, 3H), 1.98 (s, 6H), 2.00 (s, 6H), 3.98 (s, 3H), 4.42–4.44 (m, 4H), 7.47 (d, *J* = 7.2 Hz, 1H), 7.49–7.53 (m, 6H), 7.67 (dd, *J* = 7.9, 7.2 Hz, 1H), 7.70–7.76 (m, 5H), 7.89 (ddd, *J* = 8.3, 1.7, 1.0 Hz, 1H), 8.04 (s, 1H), 8.07 (ddd, *J* = 7.9, 1.7, 1.4 Hz, 1H), 8.09 (s, 1H), 8.11 (s, 1H), 8.14 (s, 1H), 8.15 (s, 2H), 8.20 (dd, *J* = 1.7, 1.4 Hz, 1H), 8.21 (t, *J* = 1.7 Hz, 1H), 8.36 (dd, *J* = 1.7, 1.4 Hz, 1H), 8.37–8.38 (m, 3H), 8.39 (dd, *J* = 1.4, 1.0 Hz, 1H), 8.43 (d, *J* = 7.9 Hz, 1H), 8.52–8.57 ppm (m, 5H); ^{13}C NMR (150 MHz, $CDCl_3$): δ = 0.1, 14.1, 22.7, 23.1, 23.2, 23.2, 23.2, 26.0, 28.7, 29.3, 29.6, 31.9, 52.3, 65.8, 88.6, 89.3, 89.4, 92.9, 93.0, 93.0, 93.7, 100.2, 103.1, 119.7, 119.8, 119.8, 120.1, 120.3, 123.6, 123.6, 123.7, 123.8, 124.3, 126.6, 126.7, 126.8, 126.9, 126.9, 126.9, 127.0, 127.0, 128.6, 129.1, 129.2, 129.2, 129.3, 129.3, 129.4, 129.6, 129.9, 130.6, 130.8, 131.0, 131.0, 131.1, 131.5, 132.1, 132.2, 132.2, 132.2, 132.4, 132.8, 135.8, 136.8, 136.9, 136.9, 136.9, 138.3, 165.4, 166.4 ppm; MS (FAB, NBA): *m/z* 1637 $[M+H]^+$; elemental analysis: calcd (%) for $C_{117}H_{106}O_6Si$: C 85.89, H 6.53; found: C 85.82, H 6.36.

16: This compound (333 mg, 0.213 mmol, 100 %) was prepared from **10** (350 mg, 0.214 mmol). M.p.: 158–159 °C (AcOEt); $[\alpha]_D^{25} = +598$ (*c* 1.00, $CHCl_3$); UV/Vis ($CHCl_3$, 5 μM): λ (ε) = 332 nm (2.1×10^5 M^{-1}cm^{-1}); CD ($CHCl_3$, 5 μM): λ ($\Delta\varepsilon$) = 297 (53), 333 (−66), 388 nm (144 M^{-1}cm^{-1}); IR (KBr): $\tilde{\nu}$ = 3287, 2204, 2112, 1722 cm^{-1}; ^{1}H NMR (600 MHz, $CDCl_3$): δ = 0.86 (t, *J* = 7.1 Hz, 6H), 1.23–1.38 (m, 20H), 1.38–1.44 (m, 4H), 1.48–1.53 (m, 4H), 1.83–1.89 (m, 4H), 1.96 (s, 6H), 1.98 (s, 6H), 2.00 (s, 6H), 3.57 (s, 1H), 3.98 (s, 3H), 4.42–4.44 (m, 4H), 7.48 (d, *J* = 7.1 Hz, 1H), 7.50–7.53 (m, 6H), 7.67 (dd, *J* = 8.4, 7.1 Hz, 1H), 7.70–7.76 (m, 5H), 7.89 (ddd, *J* = 7.6, 1.7, 1.4 Hz, 1H), 8.07 (ddd, *J* = 7.9, 1.7, 1.0 Hz, 1H), 8.08 (s, 1H), 8.11 (s, 2H), 8.14 (s, 1H), 8.16 (s, 2H), 8.20 (dd, *J* = 1.7, 1.4 Hz, 1H), 8.21 (dd, *J* = 1.7, 1.3 Hz, 1H), 8.36 (t, *J* = 1.7 Hz, 1H), 8.37–8.38 (m, 3H), 8.39 (dd, *J* = 1.7, 1.4 Hz, 1H), 8.45 (d, *J* = 8.4 Hz, 1H), 8.52–8.57 ppm (m, 5H); ^{13}C NMR (150 MHz, $CDCl_3$): δ = 14.1, 22.6, 23.2, 23.2, 23.2, 26.0, 28.7, 29.3, 29.3, 29.5, 31.9, 52.3, 65.8, 81.8, 82.4, 88.6, 89.3, 89.3, 89.4, 93.0, 93.0, 93.7, 119.3, 119.8, 119.8, 119.8, 120.1, 123.5, 123.6, 123.6, 123.8, 124.3, 126.7, 126.8, 126.8, 126.9, 126.9, 127.0, 127.0, 128.6, 129.2, 129.2, 129.2, 129.3, 129.3, 129.4, 129.6, 129.8, 129.8, 130.4, 130.6, 130.8, 130.9, 130.9, 131.0, 131.1, 131.5, 132.1, 132.2, 132.2, 132.3, 132.8, 135.8, 136.8, 136.9, 136.9, 136.9, 138.3, 165.4, 166.4 ppm; MS (FAB, NBA): *m/z* 1564 $[M]^+$; elemental analysis: calcd (%) for $C_{114}H_{98}O_6$: C 87.55, H 6.32; found: C 87.42, H 6.35.

11: This compound (418 mg, 0.190 mmol, 89 %) was prepared from **16** (333 mg, 0.213 mmol) and (*M*)-**8** (167 mg, 0.213 mmol). M.p.: 143–144 °C (chloroform/methanol); $[\alpha]_D^{22} = +556$ (*c* 1.00, $CHCl_3$); UV/Vis ($CHCl_3$, 5 μM): λ (ε) = 337 nm (3.0×10^5 M^{-1}cm^{-1}); CD ($CHCl_3$, 5 μM): λ ($\Delta\varepsilon$) = 298 (70), 337 (−86), 389 nm (202 M^{-1}cm^{-1}); IR (KBr): 2206, 2146, 1723 cm^{-1}; ^{1}H NMR (600 MHz, $CDCl_3$): δ = 0.38 (s, 9H), 0.85 (t, *J* = 6.9 Hz, 9H), 1.23–1.38 (m, 30H), 1.38–1.44 (m, 6H), 1.48–1.53 (m, 6H), 1.83–1.89 (m, 6H), 1.94 (s, 3H), 1.95 (s, 3H), 1.98 (s, 6H), 2.00 (s, 12H), 3.98 (s, 3H), 4.41–4.44 (m, 6H), 7.45 (d, *J* = 6.9 Hz, 1H), 7.47–7.52 (m, 8H), 7.67 (dd, *J* = 6.9, 7.9 Hz, 1H), 7.70–7.76 (m, 7H), 7.88 (ddd, *J* = 7.9, 1.7, 1.4 Hz, 1H), 8.03 (s, 1H), 8.06 (ddd, *J* = 7.9, 1.7, 1.4 Hz, 1H), 8.08 (s, 1H), 8.11 (s, 1H), 8.14 (s, 1H), 8.16 (s, 1H), 8.16 (s, 3H), 8.20 (t, *J* = 1.7 Hz, 1H), 8.21 (dd, *J* = 1.7, 1.3 Hz, 1H), 8.22 (t, *J* = 1.7 Hz, 1H), 8.36 (dd, *J* = 1.7, 1.3 Hz, 1H), 8.37–8.39 (m, 6H), 8.43 (d, *J* = 7.9 Hz, 1H), 8.52–8.58 ppm (m, 7H); ^{13}C NMR (150 MHz, $CDCl_3$): δ = 0.1, 14.1, 22.7, 23.1, 23.2, 23.2, 23.2, 26.0, 28.7, 29.3, 29.5, 31.9, 52.3, 65.8, 88.6, 89.3, 92.9, 93.0, 93.7,

100.1, 103.1, 119.7, 119.8, 119.8, 120.1, 120.3, 123.6, 123.6, 123.8, 124.3, 126.6, 126.7, 126.8, 126.9, 127.0, 128.6, 129.1, 129.2, 129.3, 129.4, 129.6, 129.8, 130.6, 130.8, 130.9, 131.0, 131.4, 132.1, 132.2, 132.4, 132.8, 135.8, 136.7, 136.9, 138.3, 165.4, 166.4 ppm; MS (MALDI-TOF): *m/z* calcd for $^{12}C_{157}{}^{13}CH_{144}O_8Si$: 2198.1; found: 2199.3; elemental analysis: calcd (%) for $C_{158}H_{144}O_8Si$: C 86.30, H 6.60; found: C 86.16, H 6.62.

17: This compound (368 mg, 0.173 mmol, 99%) was prepared from **11** (386 mg, 0.176 mmol). M.p.: 139–141 °C (chloroform/methanol); $[\alpha]_D^{27} = +563$ (*c* 1.00, $CHCl_3$); UV/Vis ($CHCl_3$, 5 μM): λ (ε) = 334 nm (2.7×10^5 M^{-1}cm^{-1}); CD ($CHCl_3$, 5 μM): λ ($\Delta\varepsilon$) = 298 (59), 335 (−88), 388 nm (190 M^{-1}cm^{-1}); IR (KBr): $\tilde{\nu}$ = 3305, 2206, 2101, 1723 cm^{-1}; ^{1}H NMR (600 MHz, $CDCl_3$): δ = 0.85 (t, *J* = 6.9 Hz, 9H), 1.23–1.38 (m, 30H), 1.38–1.44 (m, 6H), 1.48–1.53 (m, 6H), 1.83–1.89 (m, 6H), 1.95 (s, 6H), 1.97 (s, 6H), 2.00 (s, 12H), 3.56 (s, 1H), 3.97 (s, 3H), 4.41–4.44 (m, 6H), 7.46 (d, *J* = 7.0 Hz, 1H), 7.48–7.52 (m, 8H), 7.67 (dd, *J* = 8.3, 7.0 Hz, 1H), 7.69–7.76 (m, 7H), 7.88 (ddd, *J* = 7.6, 1.7, 1.4 Hz, 1H), 8.06 (dt, *J* = 7.9, 1.4 Hz, 1H), 8.07 (s, 1H), 8.10 (s 1H), 8.11 (s, 1H), 8.13 (s, 1H), 8.16 (s, 4H), 8.20 (dd, *J* = 1.7, 1.4 Hz, 1H), 8.21 (dd, *J* = 1.7, 1.4 Hz, 1H), 8.22 (dd, *J* = 1.7, 1.0 Hz, 1H) 8.35 (dd, *J* = 1.7, 1.4 Hz, 1H), 8.37–8.39 (m, 6H), 8.45 (d, *J* = 8.3 Hz, 1H), 8.52–8.57 ppm (m, 7H); ^{13}C NMR (150 MHz, $CDCl_3$): δ = 14.1, 22.7, 23.2, 23.2, 23.2, 26.0, 28.7, 29.3, 29.3, 29.6, 31.9, 52.3, 65.8, 81.8, 82.4, 88.6, 89.3, 89.3, 89.4, 93.0, 93.0, 93.7, 119.3, 119.8, 119.8, 119.8, 120.1, 123.5, 123.6, 123.6, 123.8, 124.3, 126.7, 126.8, 126.8, 126.9, 126.9, 127.0, 127.0, 128.6, 129.2, 129.3, 129.3, 129.4, 129.6, 129.8, 129.8, 130.4, 130.6, 130.8, 130.9, 131.0, 131.0, 131.5, 132.1, 132.2, 132.4, 132.8, 135.8, 136.8, 136.9, 136.9, 138.3, 165.4, 166.4 ppm; MS (MALDI-TOF): *m/z* calcd for $^2C_{154}{}^{13}CH_{136}O_8$: 2126.0; found: 2126.4; elemental analysis: calcd (%) for $C_{155}H_{136}O_8$: C 87.54, H 6.45; found: C 87.40, H 6.52.

12: This compound (442 mg, 0.160 mmol, 92%) was prepared from **17** (368 mg, 0.173 mmol) and (*M*)-**8** (136 mg, 0.173 mmol). M.p.: 146–148 °C (chloroform/methanol); $[\alpha]_D^{22} = +556$ (*c* 0.10, $CHCl_3$); UV/Vis ($CHCl_3$, 1 μM): λ (ε) = 338 nm (3.8×10^5 M^{-1}cm^{-1}); CD ($CHCl_3$, 5 μM): λ ($\Delta\varepsilon$) = 298 (84), 335 (−109), 390 nm (256 M^{-1}cm^{-1}); IR (KBr): $\tilde{\nu}$ = 2204, 2146, 1723 cm^{-1}; ^{1}H NMR (600 MHz, $CDCl_3$): δ = 0.38 (s, 9H), 0.85 (t, *J* = 6.9 Hz, 12H), 1.23–1.38 (m, 40H), 1.38–1.43 (m, 8H), 1.48–1.53 (m, 8H), 1.83–1.88 (m, 8H), 1.93 (s, 3H), 1.94 (s, 3H), 1.97 (s, 3H), 1.97 (s, 3H), 1.99 (s, 12H), 2.00 (s, 6H), 3.97 (s, 3H), 4.40–4.44 (m, 8H), 7.45 (d, *J* = 7.1 Hz, 1H), 7.47–7.52 (m, 10H), 7.66 (dd, *J* = 7.1, 8.1 Hz, 1H), 7.69–7.76 (m, 9H), 7.88 (ddd, *J* = 7.6, 1.7, 1.4 Hz, 1H), 8.03 (s, 1H), 8.06 (dt, *J* = 7.6, 1.4 Hz, 1H), 8.08 (s, 1H), 8.10 (s, 1H), 8.12 (s, 1H), 8.15 (s, 2H), 8.15 (s, 2H), 8.16 (s, 2H), 8.19 (dd, *J* = 1.7, 1.4 Hz, 1H), 8.20 (dd, *J* = 1.7, 1.4 Hz, 1H), 8.21–8.22 (m, 2H), 8.35 (dd, *J* = 1.7, 1.4 Hz, 1H), 8.36–8.38 (m, 8H), 8.43 (d, *J* = 7.9 Hz, 1H), 8.51–8.57 ppm (m, 9H); ^{13}C NMR (150 MHz, $CDCl_3$, 60 °C): δ = 0.12, 14.0, 22.6, 23.0, 23.1, 23.1, 26.1, 28.8, 29.3, 29.3, 29.5, 31.9, 52.2, 65.8, 88.8, 89.5, 93.0, 93.1, 93.1, 93.8, 100.2, 103.3, 119.8, 120.0, 120.0, 120.3, 120.5, 123.6, 123.7, 123.8, 124.0, 124.5, 126.7, 126.8, 126.9, 126.9, 126.9, 127.0, 128.6, 129.1, 129.2, 129.3, 129.3, 129.4, 129.7, 129.9, 130.8, 131.0, 131.1, 131.2, 131.7, 132.3, 132.3, 132.4, 132.6, 132.9, 135.8, 136.8, 137.0, 137.0, 137.0, 138.2, 165.4, 166.4 ppm; MS (MALDI-TOF): *m/z* calcd for $^{12}C_{198}{}^{13}CH_{182}O_{10}Si$: 2760.4; found: 2761.7; elemental analysis: calcd (%) for $C_{199}H_{182}O_{10}Si$: C 86.55, H 6.64; found: C 86.45, H 6.69.

18: This compound (429 mg, 0.160 mmol, 99%) was prepared from **12** (442 mg, 0.160 mmol). M.p.: 148–150 °C (chloroform/methanol); $[\alpha]_D^{22} = +562$ (*c* 0.10, $CHCl_3$); UV/Vis ($CHCl_3$, 1 μM): λ (ε) = 338 nm (3.3×10^5 M^{-1}cm^{-1}); CD ($CHCl_3$, 5 μM): λ ($\Delta\varepsilon$) = 297 (77), 336 (−95), 389 nm (232 M^{-1}cm^{-1}); IR (KBr): $\tilde{\nu}$ = 3306, 2206, 2103, 1723 cm^{-1}; ^{1}H NMR (600 MHz, $CDCl_3$): δ = 0.85 (t, *J* = 6.9 Hz, 12H), 1.22–1.37 (m, 40H), 1.38–1.43 (m, 8H), 1.47–1.52 (m, 8H), 1.82–1.88 (m, 8H), 1.94 (s, 3H), 1.95 (s, 3H), 1.96 (s, 3H), 1.97 (s, 3H), 1.98 (s, 12H), 2.00 (s, 6H), 3.56 (s, 1H), 3.97 (s, 3H), 4.40–4.44 (m, 8H), 7.46 (d, *J* = 7.2 Hz, 1H), 7.48–7.52 (m, 10H), 7.67 (dd, *J* = 7.9, 7.2 Hz, 1H), 7.69–7.76 (m, 9H), 7.88 (dt, *J* = 6.2, 1.4 Hz, 1H), 8.05 (ddd, *J* = 7.3, 1.4, 1.0 Hz, 1H), 8.06 (s, 1H), 8.09 (s, 1H), 8.09 (s, 1H), 8.12 (s, 1H), 8.14 (s, 2H), 8.15 (s, 2H), 8.16 (s, 2H), 8.19 (t, *J* = 1.4 Hz, 1H), 8.20 (dd, *J* = 1.7, 1.4 Hz, 1H), 8.21 (t, *J* = 1.7 Hz, 1H), 8.22 (dd, *J* = 1.7, 1.4 Hz, 1H), 8.34 (dd, *J* = 1.7, 1.4 Hz, 1H), 8.35–8.38 (m, 8H), 8.44 (d, *J* = 7.9 Hz, 1H), 8.51–8.57 ppm (m, 9H); ^{13}C NMR (150 MHz, $CDCl_3$, 60 °C): δ = 14.0, 22.6, 23.1, 23.1, 23.1, 26.1, 28.8, 29.0, 29.3, 29.3, 29.5, 31.9, 52.2, 65.8, 82.0, 82.3, 88.8, 89.5, 89.5, 93.1, 93.1, 93.8, 119.6, 119.9, 120.0, 120.0, 120.2, 123.6, 123.7, 123.7, 124.0, 124.5, 126.8, 126.9, 126.9, 127.0, 127.0, 127.0, 128.6, 129.2, 129.2, 129.2, 129.3, 129.4, 129.7, 129.8, 129.9, 130.5, 130.8, 130.9, 131.0, 130.1, 131.2, 131.7, 132.3, 132.4, 132.5, 132.9, 135.7, 136.9, 137.0, 137.0, 137.0, 138.2, 165.4, 166.3 ppm; MS (MALDI-TOF): *m/z* calcd for $^{12}C_{195}{}^{13}CH_{174}O_{10}$: 2688.3; found: 2689.1; elemental analysis: calcd (%) for $C_{196}H_{174}O_{10}$: C 87.53, H 6.52; found: C 87.71, H 6.44.

13: This compound (104 mg, 0.0313 mmol, 82%) was prepared from **18** (103 mg, 0.0383 mmol) and (*M*)-**8** (30 mg, 0.0383 mmol). M.p.: 159–160 °C (chloroform/methanol); $[\alpha]_D^{22} = -4600$ (*c* 0.10, trifluoromethylbenzene, within 1 h of dissolution); UV/Vis (trifluoromethylbenzene, 5 μM, within 5 min of dissolution): λ (ε) = 329 nm (2.4×10^5 M^{-1}cm^{-1}); CD ($CHCl_3$, 5 μM, 1 min after dissolution): λ ($\Delta\varepsilon$) = 325 (974), 366 (−1530), 385 (−980), 391 nm (−1030 M^{-1}cm^{-1}); IR (KBr): $\tilde{\nu}$ = 2208, 2147, 1722 cm^{-1}; H NMR (600 MHz, $CDCl_3$, 1 mM, observed at 60 °C after heating at 60 °C for 15 min): δ = 0.38 (s, 9H), 0.85 (t, *J* = 6.9 Hz, 15H), 1.23–1.38 (m, 50H), 1.38–1.45 (m, 10H), 1.47–1.53 (m, 10H), 1.82–1.88 (m, 10H), 1.94 (s, 3H), 1.95 (s, 3H), 1.97 (s, 3H), 1.98 (s, 3H), 1.99 (s, 24H), 3.96 (s, 3H), 4.40–4.43 (m, 10H), 7.43 (d, *J* = 7.2 Hz, 1H), 7.45–7.49 (m, 12H), 7.64 (dd, *J* = 8.4, 7.2 Hz, 1H), 7.67–7.73 (m, 11H), 7.86 (dt, *J* = 7.8, 1.2 Hz, 1H), 8.00 (s, 1H), 8.04 (dt, *J* = 7.8, 1.2 Hz, 1H), 8.06 (s, 1H), 8.08 (s, 1H), 8.11 (s, 1H), 8.13 (s, 2H), 8.13 (s, 2H), 8.14 (s, 2H), 8.14 (s, 2H), 8.17 (t, *J* = 1.8 Hz, 1H), 8.18 (dd, *J* = 1.8, 1.2 Hz, 1H), 8.18–8.19 (m, 3H), 8.33 (dd, *J* = 1.8, 1.2 Hz, 1H), 8.34–8.37 (m, 10H), 8.42 (d, *J* = 8.4 Hz, 1H), 8.50–8.55 ppm (m, 11H); ^{13}C NMR (150 MHz, $CDCl_3$, 5 mM, observed at 60 °C after heating at 60 °C for 30 min): δ = 0.1, 14.0, 22.6, 23.0, 23.07, 23.1, 23.1, 26.1, 28.9, 29.3, 29.3, 29.6, 31.9, 52.2, 65.9, 88.0, 89.5, 89.5, 89.5, 9.54, 93.0, 93.1, 93.1, 93.1, 93.8, 119.9, 120.0, 120.1, 120.3, 120.6, 123.7, 123.7, 123.7, 123.8, 124.0, 124.5, 124.5, 124.6, 126.8, 126.9, 126.9, 127.0, 127.0, 127.0, 127.0, 127.1, 128.6, 129.1, 129.2, 129.3, 129.3, 129.3, 129.5, 129.7, 130.0, 130.9, 131.0, 131.1, 131.2, 131.2, 131.2, 131.2, 131.8, 131.8, 132.3, 132.4, 132.4, 132.5, 132.6, 132.9, 135.8, 136.9, 137.0, 137.0, 137.1, 137.1, 138.3, 165.4, 166.4 ppm; MS (MALDI-TOF): *m/z* calcd for $^{12}C_{238}{}^{13}C_2H_{220}O_{12}Si$: 3323.6; found: 3323.9; elemental analysis: calcd (%) for $C_{240}H_{220}O_{12}Si$: C 86.71, H 6.67; found: C 86.59, H 6.53.

19: This compound (318 mg, 0.0978 mmol, 97%) was prepared from **13** (334 mg, 0.100 mmol). M.p.: 154–156 °C (chloroform/methanol); $[\alpha]_D^{22} = -4600$ (*c* 0.10, trifluoromethylbenzene, within 1 h of dissolution); UV/Vis (trifluoromethylbenzene, 5 μM, within 5 min of dissolution); λ (ε) = 331 nm (2.4×10^5 M^{-1}cm^{-1}); CD ($CHCl_3$, 5 μM, 1 min after dissolution): λ ($\Delta\varepsilon$) = 326 (1030), 366 (−1600), 385 (−1060), 391 nm (−1120 M^{-1}cm^{-1}); IR (KBr): $\tilde{\nu}$ = 3303, 2208, 2100, 1723 cm^{-1}; ^{1}H NMR (600 MHz, $CDCl_3$, 1 mM, observed at 60 °C after heating at 60 °C for 15 min): δ = 0.85 (t, *J* = 7.1 Hz, 15H), 1.22–1.37 (m, 50H), 1.38–1.43 (m, 10H), 1.47–1.53 (m, 10H), 1.81–1.88 (m, 10H), 1.95 (s, 3H), 1.95 (s, 3H), 1.97 (s, 3H), 1.98 (s, 3H), 1.99 (s, 24H), 3.53 (s, 1H), 3.96 (s, 3H), 4.41–4.43 (m, 10H), 7.44 (d, *J* = 7.2 Hz, 1H), 7.46–7.49 (m, 12H), 7.64 (dd, *J* = 8.1, 7.2 Hz, 1H), 7.66–7.73 (m, 11H), 7.86 (ddd, *J* = 8.1, 1.5, 1.2 Hz, 1H), 8.04 (ddd, *J* = 6.4, 1.8, 1.1 Hz, 1H), 8.04 (s, 1H), 8.07 (s, 1H), 8.08 (s, 1H), 8.10 (s, 1H), 8.13 (s, 2H), 8.13 (s, 2H), 8.14 (s, 4H), 8.16 (dd, *J* = 1.7, 1.4 Hz, 1H), 8.18 (dd, *J* = 1.7, 1.6 Hz, 1H), 8.18–8.19 (m, 3H), 8.33 (dd, *J* = 1.6, 1.5 Hz, 1H), 8.33–8.36 (m, 10H), 8.43 (d, *J* = 8.1 Hz, 1H), 8.50–8.55 ppm (m, 11H); ^{13}C NMR (150 MHz, $CDCl_3$, 5 mM, observed at 60 °C after heating at 60 °C for 30 min): δ = 14.0, 22.6, 23.1, 23.1, 26.1, 28.9, 29.3, 29.3, 29.6, 31.9, 52.2, 65.8, 82.0, 82.3, 88.7, 89.5, 93.1, 93.1, 93.8, 119.6, 119.8, 120.0, 120.1, 120.3, 123.7, 123.7, 123.7, 124.0, 124.5, 126.9, 127.0, 127.0, 127.0, 127.0, 127.1, 128.6, 129.2, 129.3, 130.0, 129.3, 129.5, 129.7, 129.9, 130.0, 130.5, 130.9, 131.0, 131.1, 131.2, 131.2, 131.8, 132.4, 132.4, 132.6, 132.9, 135.8, 136.9, 137.0, 137.1, 138.3, 165.4, 166.4 ppm; MS (MALDI-TOF): *m/z* calcd for $^{12}C_{235}{}^{13}C_2H_{212}O_{12}$: 3251.6; found: 3252.3; elemental analysis: calcd (%) for $C_{237}H_{212}O_{12}$: C 87.53, H 6.57; found: C 87.49, H 6.53.

14: This compound (64 mg, 0.0165 mmol, 71%) was prepared from **19** (75 mg, 0.0231 mmol) and (*M*)-**8** (18.1 mg, 0.0231 mmol). M.p.: 164–166 °C (chloroform/methanol); $[\alpha]_D^{24} = -5018$ (*c* 0.10, trifluoromethylbenzene, within 1 h of dissolution); UV/Vis (trifluoromethylbenzene, 5 μM, within 5 min of dissolution): λ (ε) = 329 nm (2.8×10^5 M^{-1}cm^{-1}); CD ($CHCl_3$, 5 μM, 1 min after dissolution): λ ($\Delta\varepsilon$) = 327 (1540), 366 (−2350),

385 (−1600), 391 nm (−1710 $M^{-1}cm^{-1}$); IR (KBr): 2208, 2146, 1724 cm^{-1}; ^1H NMR (600 MHz, $CDCl_3$, 3 mM, observed at 60 °C after heating at 60 °C for 1 h): $\delta = 0.38$ (s, 9H), 0.85 (t, $J = 7.1$ Hz, 18H), 1.22–1.36 (m, 60H), 1.41 (quin, $J = 7.1$ Hz, 12H), 1.50 (quin, $J = 7.7$ Hz, 12H), 1.85 (quin, $J = 7.4$ Hz, 12H), 1.94 (s, 3H), 1.95 (s, 3H), 1.968 (s, 3H), 1.974 (s, 3H), 1.99 (s, 30H), 3.95 (s, 3H), 4.40–4.43 (m, 12H), 7.43 (d, $J = 7.0$ Hz, 1H), 7.45–7.49 (m, 14H), 7.64 (dd, $J = 8.2$, 7.2 Hz, 1H), 7.66–7.72 (m, 13H), 7.85 (ddd, $J = 8.0$, 1.6, 1.2 Hz, 1H), 8.00 (s, 1H), 8.03 (ddd, $J = 7.9$, 1.7, 1.3 Hz, 1H), 8.05 (s, 1H), 8.07 (s, 1H), 8.09 (s, 1H), 8.11 (s, 2H), 8.12 (s, 2H), 8.12 (s, 6H), 8.16 (t, $J = 1.6$ Hz, 1H), 8.17 (dd, $J = 1.7$, 1.6 Hz, 1H), 8.17- 8.18 (m, 4H), 8.32–8.36 (m, 13H), 8.42 (d, $J = 8.0$ Hz, 1H), 8.49–8.55 ppm (m, 13H); ^{13}C NMR (150 MHz, $CDCl_3$, 3 mM, observed at 60 °C after heating at 60 °C for 30 min): $\delta = 14.0$, 22.6, 23.1, 26.1, 28.9, 29.4, 29.6, 31.9, 52.2, 65.8, 88.8, 89.5, 93.0, 93.1, 93.2, 93.8, 100.3, 119.9, 120.0, 120.1, 120.3, 120.6, 123.7, 123.8, 123.8, 124.0, 124.5, 124.6, 126.8, 126.9, 126.9, 127.0. 127.0, 127.0, 127.1, 128.6, 129.1, 129.2, 129.3, 129.3, 129.3, 129.5, 129.7, 130.0, 131.0, 131.2, 131.2, 131.8, 132.3, 132.4, 132.4, 132.6, 132.9, 135.8, 136.9, 137.0, 137.1, 137.1, 138.3, 165.5, 166.4 ppm; MS (MALDI-TOF): *m/z* calcd for $^{12}C_{279}{}^{13}C_2H_{258}O_{14}Si$: 3885.9; found: 3887.8; elemental analysis: calcd (%) for $C_{281}H_{258}O_{14}Si$: C 86.83, H 6.69; found: C 86.55, H 6.86.

20: Under argon atmosphere, a mixture of 3-iodobenzoic acid (500 mg, 2.02 mmol) and thionyl chloride (3 mL) was heated at reflux for 1 h. After cooling to room temperature, the solvent was removed under reduced pressure, and the resulting acid chloride was azeotropically dried by adding dichloromethane (3 mL) and evaporating the mixture twice. Next, dichloromethane (3 mL), triethylamine (0.56 mL), and 1,16-hexadecanediol (261 mg, 1.01 mmol) were added at 0 °C. After the mixture was stirred at room temperature for 3 h, the reaction was quenched by adding saturated aqueous ammonium chloride, and the organic materials were extracted with ethyl acetate. The organic layer was washed with water and brine and dried over magnesium sulfate. After removal of the solvents under reduced pressure, silica-gel chromatography (hexane/toluene = 1:1) gave **20** (438 mg, 0.610 mmol, 60 %). M.p.: 69–70 °C (ethanol); IR (KBr): $\tilde{\nu} = 1721$ cm^{-1}; ^1H NMR (400 MHz, $CDCl_3$): $\delta = 1.23$–1.46 (m, 24H), 1.76 ($J = 6.8$ Hz, 4H), 4.31 (t, $J = 6.7$H, 4H), 7.18 (t, $J = 7.8$ Hz, 2H), 7.88 (ddd, $J = 7.8$, 1.8, 1.1 Hz, 2H), 8.00 (ddd, $J = 7.8$, 1.7, 1.1 Hz, 2H), 8.37 ppm (dd, $J = 1.8$, 1.7 Hz, 2H); ^{13}C NMR (150 MHz, $CDCl_3$): $\delta = 26.0$, 28.6, 29.2, 29.5, 29.6, 29.6, 29.6, 65.6, 93.8, 128.7, 130.0, 132.4, 138.4, 141.6, 165.2 ppm; LRMS (EI, 70 eV): *m/z* (%): 718 $[M]^+$ (56 %), 231 $[M-(CH_2)_{16}O_2CC_6H_4I]^+$ (100); HRMS (EI): *m/z* calcd for $C_{30}H_{40}I_2O_4$: 718.1016 $[M]^+$; found: 718.1015.

2: Under argon atmosphere, a mixture of **20** (5.5 mg, 7.66 μmol), tris(dibenzylideneacetone)dipalladium(0) chloroform adduct (4.0 mg, 3.86 μmol), cuprous iodide (8.8 mg, 0.0462 mmol), trimesitylphosphine (9.0 mg, 0.0232 mmol), tetrabutylammonium iodide (120 mg, 0.325 mmol), triethylamine (0.5 mL), and *N,N*-dimethylformamide (5 mL) was freeze-evacuated three times. A solution of **19** (50 mg, 0.0154 mmol) in *N,N*-dimethylformamide (5 mL) was freeze-evacuated three times and added dropwise to the above solution. The mixture was stirred for 2 h at 45 °C. The reaction was quenched by adding saturated aqueous ammonium chloride, and the organic materials were extracted with toluene. The organic layer was washed with brine and dried over magnesium sulfate. The solvents were evaporated under reduced pressure, and separation by recycling GPC gave **2** (28.3 mg, 4.06 μmol, 53 %). M.p.: 163–165 °C (chloroform/methanol); $[\alpha]_D^{27} = -4814$ (*c* 0.10, trifluoromethylbenzene, within 1 h of dissolution); UV/Vis (trifluoromethylbenzene, 1 μM, within 5 min of dissolution): λ (ε) = 331 nm (4.7×10^5 $M^{-1}cm^{-1}$); CD ($CHCl_3$, 5 μM, 1 min after dissolution) λ ($\Delta\varepsilon$) = 328 (2680), 366 (−4280), 385 (−2790), 390 nm (−2850 $M^{-1}cm^{-1}$); IR (KBr): $\tilde{\nu} = 2206$, 1721 cm^{-1}; ^1H NMR (600 MHz, $[D_8]$toluene, 1 mM, observed at 100 °C after heating at 100 °C for 2 h): $\delta = 0.86$ (t, $J = 7.2$ Hz, 30H), 1.21–1.40 (m, 164H), 1.60–1.70 (m, 24H), 1.88 (s, 12H), 1.89 (s, 12H), 1.90 (s, 48H), 3.59 (s, 6H), 4.24 (t, $J = 6.9$ Hz, 4H), 4.28–4.31 (m, 24H), 7.07–7.12 (m, 4H), 7.19–7.24 (m, 26H), 7.45–7.52 (m, 24H), 7.62–7.65 (m, 4H), 7.89 (s, 2H), 7.92 (s, 2H), 7.92 (s, 2H), 7.93 (ddd, $J = 8.0$, 1.5, 1.3 Hz, 2H), 7.94 (s, 2H), 7.96 (s, 4H), 7.97 (s, 4H), 7.97 (s, 8H), 8.01 (ddd, $J =$ 7.6, 1.6, 1,2 Hz, 2H), 8.21–8.23 (m, 10H), 8.47–8.48 (m, 2H), 8.53–8.56 (m, 20H), 8.62 (d, $J = 7.9$ Hz, 2H), 8.63 (d, $J = 8.0$ Hz, 2H), 8.65–8.68 ppm (m, 20H); ^{13}C NMR (150 MHz, $[D_8]$THF, 1 mM, observed at 60 °C after heating at 60 °C for 2 h); $\delta = 14.3$, 14.5, 23.3, 23.4, 23.6, 23.7, 27.0, 27.2, 29.7, 30.2, 30.2, 30.5, 30.5, 30.7, 32.8, 33.0, 52.3, 65.0, 65.9, 66.3, 89.4, 90.2, 93.8, 94.5, 120.9, 121.0, 121.2, 124.6, 125.4, 127.8, 127.8, 127.9, 127.9, 129.5, 129.6, 130.1, 130.2, 130.5, 130.6, 130.9, 132.0, 132.3, 132.9, 133.0, 133.2, 133.3, 133.3, 136.3, 136.4, 137.8, 137.9, 138.9, 165.4, 165.9, 166.4 ppm; MS (MALDI-TOF): *m/z* calcd for $^{12}C_{499}{}^{13}C_5H_{462}O_{28}$: 6966.5; found: 6966.8; elemental analysis: calcd (%) for $C_{504}H_{462}O_{28}$: C 86.89, H 6.68; found: C 86.66, H 6.71.

21: A mixture of 1-ethynyl-4-iodobenzene (125 mg, 0.546 mmol), cuprous chloride (31.4 mg, 0.317 mmol), *N,N,N′,N′*-tetramethylethylenediamine (0.3 mL), and acetone (5 mL) was stirred for 30 min at room temperature with bubbling of oxygen. The reaction was quenched by adding water, and the organic materials were extracted with toluene. The organic layer was washed with water and brine and dried over magnesium sulfate. The solvents were removed under reduced pressure, and silica-gel chromatography gave **21** (109 mg, 0.240 mmol, 88 %). M.p.: 238–240 °C (toluene); IR (KBr): $\tilde{\nu} = 2149$ cm^{-1}; ^1H NMR (400 MHz, $CDCl_3$): $\delta = 7.22$ (d, $J =$ 8.6 Hz, 4H), 7.68 (d, $J = 8.6$ Hz, 4H); ^{13}C NMR (150 MHz, $CDCl_3$): $\delta =$ 75.1, 81.2, 95.7, 121.1, 133.8, 137.7 ppm; LRMS (EI, 70 eV) *m/z* (%): 454 $[M]^+$ (100), 327 $[M-I]^+$ (14), 200 $[M-2I]^+$ (16); HRMS (EI); *m/z* calcd for $C_{16}H_8I_2$: 453.8715; found: 453.8699.

3: Under argon atmosphere, a mixture of **21** (4.9 mg, 0.0108 μmol), tris(dibenzylideneacetone)dipalladium(0) chloroform adduct (2.8 mg, 2.17 μmol), cuprous iodide (6.1 mg, 0.0320 mmol), trimesitylphosphine (6.3 mg, 0.0162 mmol), tetrabutylammonium iodide (79.4 mg, 0.215 mmol), triethylamine (0.5 mL), and *N,N*-dimethylformamide (5 mL) was freeze-evacuated three times. A solution of **19** (70 mg, 0.0215 mmol) in *N,N*-dimethylformamide (5 mL) was freeze-evacuated three times and added dropwise to the above solution. The mixture was stirred for 2 h at 45 °C. The reaction was quenched by adding saturated aqueous ammonium chloride, and the organic materials were extracted with toluene. The organic layer was washed with brine and dried over magnesium sulfate. The solvents were evaporated under reduced pressure, and separation by recycling GPC gave **3** (32,5 mg, 4.85 μmol, 45 %). M.p.: 197–199 °C (chloroform/methanol); $[\alpha]_D^{27} = -3686$ (*c* 0.010, trifluoromethylbenzene, within 1 h of dissolution); UV/Vis (trifluoromethylbenzene, 1 μM, within 5 min of dissolution): λ (ε) = 334 nm (3.3×10^5 $M^{-1}cm^{-1}$); CD ($CHCl_3$, 5 μM, 1 min after dissolution); λ ($\Delta\varepsilon$) = 334 (2590), 372 (−3460), 383 (−3090), 392 nm (−3410 $M^{-1}cm^{-1}$); IR (KBr): $\tilde{\nu} = 2206$, 1722 cm^{-1}; ^1H NMR (600 MHz, $[D_8]$toluene, 1 mM, observed at 100 °C after heating at 100 °C for 2 h): $\delta = 0.86$ (t, $J = 6.9$ Hz, 30H), 1.20–1.40 (m, 140H, m), 1.64–1.72 (quin, $J = 6.6$ Hz, 20H), 1,88 (s, 6H), 1.89 (s, 12H), 1.91 (s, 54H), 3.59 (s, 6H), 4.29–4.31 (m, 20H), 7.19–7.24 (m, 26H), 7.34 (d, $J = 7.8$ Hz, 4H), 7.44–7.52 (m, 28H) 7.63 (d, $J = 7.8$ Hz, 2H), 7.90–8.10 (br, 26H), 8.21–8.23 (m, 10H), 8.48 (m, 2H), 8.53–8.57 (m, 20H), 8.61 (d, $J = 7.8$ Hz, 2H), 8.63 (d, $J = 7.8$ Hz, 2H), 8.66–8.68 ppm (m, 20H); ^{13}C NMR (150 MHz, $[D_8]$THF, 1 mM, observed at 60 °C after heating at 60 °C for 2 h): $\delta = 14.3$, 23.3, 23.4, 25.8, 27.0, 29.7, 30.2, 30.2, 30.5, 30.5, 32.8, 52.3, 66.3, 76.4, 78.9, 79.1, 79.3, 89.4, 90.2, 93.7, 93.8, 94.5, 120.9, 121.0, 121.2, 121.2, 123.7, 124.6, 124.8, 125.5, 127.6, 127.7, 127.8, 127.8, 127.9, 128.0, 129.0, 129.6, 130.1, 130.2, 130.2, 130.6, 130.9, 132.0, 132.1, 132.3, 132.6, 133.0, 133.0, 133.3, 133.3, 133.4, 136.4, 137.8, 137.9, 138.9, 165.4, 166.4 ppm; MS (MALDI-TOF): *m/z* calcd for $^{12}C_{486}{}^{13}C_4H_{430}O_{24}$: 6701.2; found: 6702.3; elemental analysis: calcd (%) for $C_{490}H_{430}O_{24}$: C 87.80, H 6.47; found: C 87.12, H 6.55.

Determination of Thermodynamic Parameters

The equilibrium constant K_{eq} of **2** and **3** is defined as shown in Equation (1), in which $[R_{eq}]$ and $[H_{eq}]$ are the concentrations of the random coil and helix, respectively, at equilibrium.

$$K_{eq} = [R_{eq}]/[H_{eq}] \quad (1)$$

$\Delta\varepsilon$ at equilibrium ($\Delta\varepsilon_{eq}$) is described in Equation (2) with the initial helix concentration $[H_0]$.

$$\Delta\varepsilon_{eq} = \Delta\varepsilon_H([H_{eq}]/[H_0]) + \Delta\varepsilon_R([R_{eq}]/[H_0]) \quad (2)$$

The initial helix concentration $[H_0]$ is defined as shown in Equation (3).

$$[H_0] = [H_{eq}] + [R_{eq}] \quad (3)$$

The rearrangement of Equation 3 gives Equation (4)

$$[R_{eq}] = [H_0] - [H_{eq}] \quad (4)$$

Substitution of $[R_{eq}]$ into Equation 2 and solving for $[H_{eq}]$ gives Equation (5).

$$[H_{eq}] = [H_0](\Delta\varepsilon_{eq} - \Delta\varepsilon_R)/(\Delta\varepsilon_H - \Delta\varepsilon_R) \quad (5)$$

The $[R_{eq}]$ and $[H_{eq}]$ values for **2** at each temperature were obtained by using $\Delta\varepsilon_{eq} = +100$ (60 °C), -500 (55 °C), -1150 (50 °C), and $-2300\,M^{-1}cm^{-1}$ (45 °C), $\Delta\varepsilon_H = -4090\,M^{-1}cm^{-1}$, and $\Delta\varepsilon_R = 300\,M^{-1}cm^{-1}$ (Figure 10), and K_{eq} was calculated by using Equation (1), from which ΔG was obtained (Table 1). The van't Hoff plots provided $\Delta H = (194 \pm 19)$ kJ mol^{-1} and $\Delta S = (0.61 \pm 0.06)$ kJ mol^{-1} K^{-1} (Figure 21).

Determination of the Activation Energy for Unfolding

The unfolding process of **2** and **3** is described in Equation (6).

Table 1. Equilibrium constant K_{eq} and free energy ΔG of **2** (5 μM) in toluene at various temperatures.

	60 °C	55 °C	50 °C	45 °C
K_{eq}	21 ± 1	4.5 ± 0.1	2.0 ± 0.1	0.69 ± 0.01
ΔG [kJmol^{-1}]	−8.4 ± 0.2	−4.1 ± 0.1	+1.9 ± 0.1	+0.98 ± 0.05

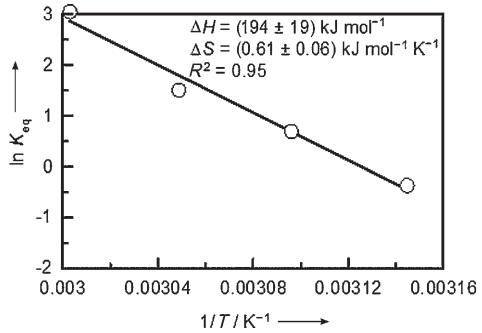

Figure 21. van't Hoff plot of **2** (5 μM) in toluene.

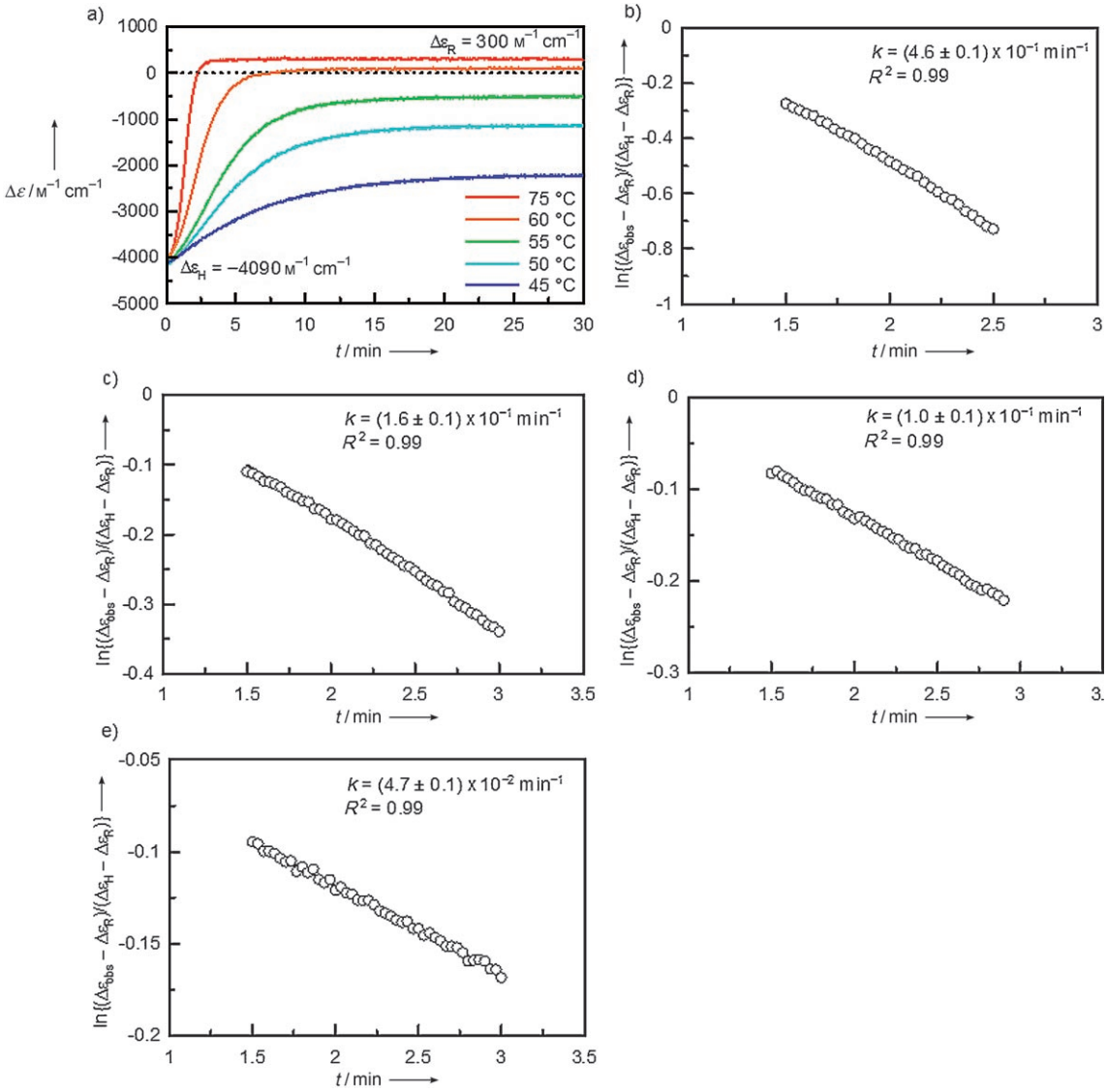

Figure 22. a) Time dependence of $\Delta\varepsilon$ at 370 nm for **2** (5 μM) in toluene at 75, 60, 55, 50, and 45 °C. $\Delta\varepsilon_H = -4090\,M^{-1}cm^{-1}$ and $\Delta\varepsilon_R = 300\,M^{-1}cm^{-1}$ were obtained at 75 °C. Plots of $\ln\{(\Delta\varepsilon_{obs} - \Delta\varepsilon_R)\}/(\Delta\varepsilon_H - \Delta\varepsilon_R)\}$ of **2** versus time after heating at b) 60 °C, c) 55 °C, d) 50 °C, and e) 45 °C.

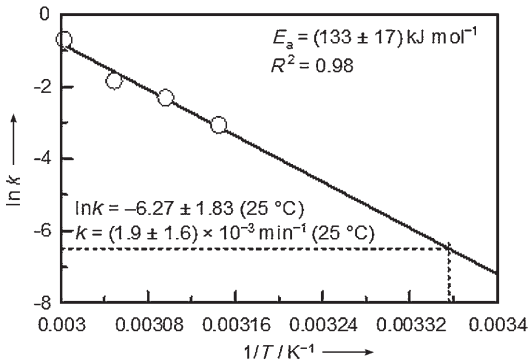

Figure 23. Arrhenius plot for the unfolding of **2** in toluene.

$$\text{Helix(H)} \xrightarrow{k} \text{Randomcoil(R)} \tag{6}$$

The observed $\Delta\varepsilon$ ($\Delta\varepsilon_{obs}$) is described as shown in Equation (7), in which [H] is the helix concentration and [R] is the random coil concentration.

$$\Delta\varepsilon_{obs} = \Delta\varepsilon_H([H]/[H_0]) + \Delta\varepsilon_R([R]/[H_0]) \tag{7}$$

The initial helix concentration [H_0] is defined as shown in Equation (8).

$$[H_0] = [H] + [R] \tag{8}$$

The rearrangement of Equation (8) gives Equation (9).

$$[H] = [H_0] - [R] \tag{9}$$

Substitution for [H] in Equation (7) and solving for [R] gives Equation (10).

$$[R] = [H_0](\Delta\varepsilon_H - \Delta\varepsilon_{obs})/(\Delta\varepsilon_H - \Delta\varepsilon_R) \tag{10}$$

From Equation (10), conversion (%) is calculated by using Equation (11).

$$\text{Conversion } (\%) = [R]/[H]_0 \times 100 = (\Delta\varepsilon_H - \Delta\varepsilon_{obs})/(\Delta\varepsilon_H - \Delta\varepsilon_R) \times 100 \tag{11}$$

By assuming a pseudo-first-order reaction, the unfolding rate is defined as shown in Equation (12).

$$\ln\{([H_0] - [R])/[H_0]\} = -kt \tag{12}$$

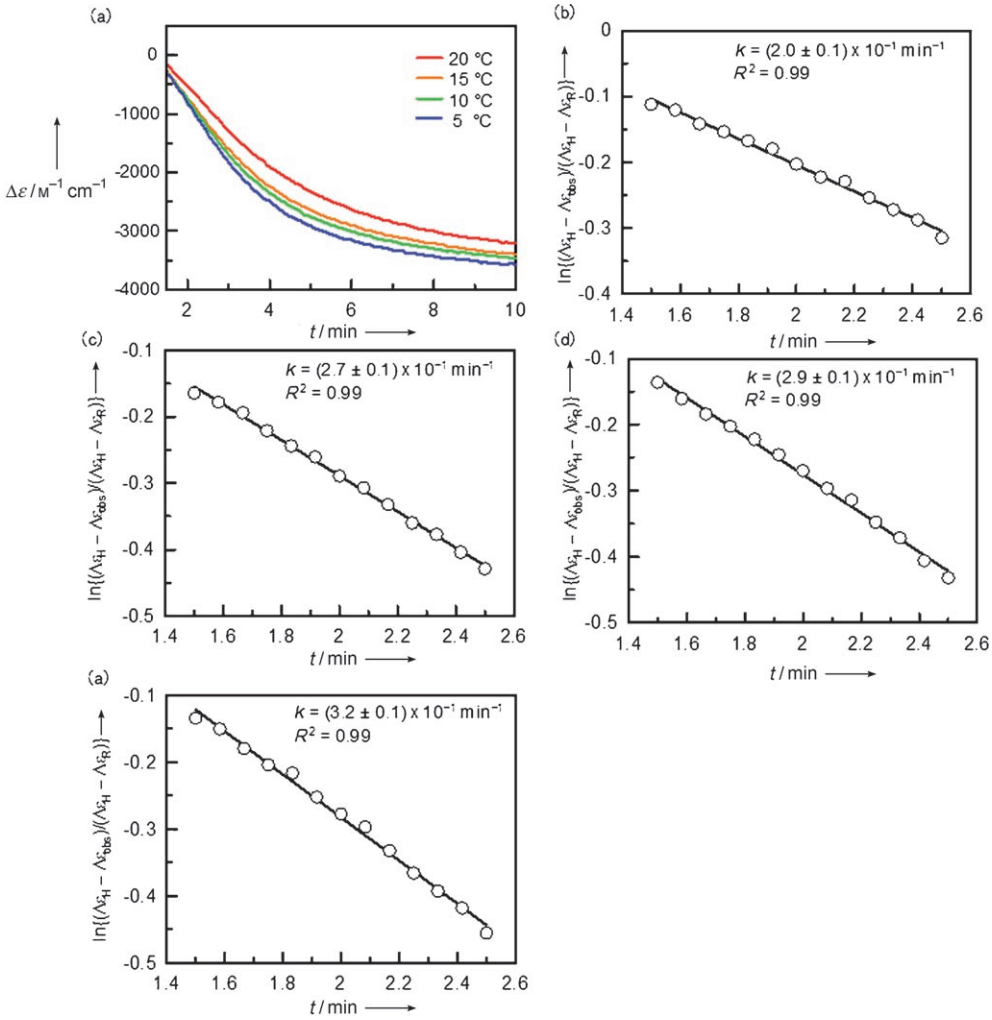

Figure 24. a) Time dependence of Δε at 370 nm for **2** (5 μM) in toluene at 20, 15, 10, and 5 °C after heating at 75 °C for 30 min. Plots of ln{($\Delta\varepsilon_H - \Delta\varepsilon_{obs}$)}/($\Delta\varepsilon_H - \Delta\varepsilon_R$)} of **2** versus time after cooling at b) 20 °C, c) 15 °C, d) 10 °C, and e) 5 °C.

Substitution of Equation (10) into Equation (12) gives Equation (13).

$$\ln\{(\Delta\varepsilon_{obs}-\Delta\varepsilon_R)/(\Delta\varepsilon_H-\Delta\varepsilon_R)\} = -kt \quad (13)$$

A 5-μM solution was prepared by dissolving compound **2** in toluene at 25 °C, and the solution was heated at 60, 55, 50, or 45 °C within 1 min of dissolution. The unfolding process was monitored by $\Delta\varepsilon$ at 370 nm (Figure 22a). $\Delta\varepsilon_H = -4090\,M^{-1}cm^{-1}$ and $\Delta\varepsilon_R = 300\,M^{-1}cm^{-1}$ were obtained at 75 °C. Then, by using $\Delta\varepsilon$ values at less than 30% conversion, $\ln\{(\Delta\varepsilon_{obs}-\Delta\varepsilon_R)/(\Delta\varepsilon_H-\Delta\varepsilon_R)\}$ was plotted against time after heating (Figure 22b–e). As the unfolding was fast at 60 °C, $\Delta\varepsilon$ values at less than 55% conversion was employed. The slopes of the plots were calculated by the least-squares method to give $k = (4.6\pm0.1)\times10^{-1}$ (60 °C), $(1.6\pm0.1)\times10^{-1}$ (55 °C), $(1.0\pm0.1)\times10^{-1}$ (50 °C), and $(4.7\pm0.1)\times10^{-2}\,min^{-1}$ (45 °C) (Figure 22).

To determine the activation energy of the unfolding process of **2**, ln*k* was plotted against $1/T$ (Arrhenius plot), and the slope of the plot was calculated by the least-squares method to give the activation energy $E_a = (133\pm17)\,kJ\,mol^{-1}$ for the unfolding of **2** (Figure 23).The rate constant $k = (1.9\pm1.6)\times10^{-3}\,min^{-1}$ at 25 °C was also estimated by using the Arrhenius plots.

The rate constant *k* and activation energy for folding [Eq. (14)] were determined.

$$\text{Randomcoil(R)} \xrightarrow{k} \text{Helix(H)} \quad (14)$$

As for the folding process of **2** and **3**, the rate is defined as shown in Equation (15).

$$\ln\{([R_0]-[H])/[R_0]\} = -kt \quad (15)$$

From Equations (7) and (8), [H] is described as shown in Equation (16).

$$[H] = [R_0](\Delta\varepsilon_{obs}-\Delta\varepsilon_R)/(\Delta\varepsilon_H-\Delta\varepsilon_R) \quad (16)$$

From Equation (16), conversion (%) is calculated by using Equation (17).

$$\text{Conversion}\ (\%) = [H]/[R]_0 \times 100 = (\Delta\varepsilon_{obs}-\Delta\varepsilon_R)/(\Delta\varepsilon_H-\Delta\varepsilon_R) \times 100 \quad (17)$$

Substitution of Equation (16) into Equation (11) gives Equation (18).

$$\ln\{(\Delta\varepsilon_H-\Delta\varepsilon_{obs})/(\Delta\varepsilon_H-\Delta\varepsilon_R)\} = -kt \quad (18)$$

A 5-μM solution of **2** in toluene was heated at 75 °C for 30 min for **2** to unfold completely to the random-coil structure, and the time dependence of $\Delta\varepsilon$ at 370 nm was measured at 20, 15, 10, and 5 °C for the folding process (Figure 24). $\Delta\varepsilon_R = 300\,M^{-1}cm^{-1}$ and $\Delta\varepsilon_H = -4090\,M^{-1}cm^{-1}$ were obtained at 5 °C (Figure 13). Then, by using $\Delta\varepsilon$ values at less than 40% conversion, $\ln\{(\Delta\varepsilon_H-\Delta\varepsilon_{obs})/(\Delta\varepsilon_H-\Delta\varepsilon_R)\}$ was plotted against time after cooling, and the slopes of the plots were calculated by the least-squares method to give $k = (2.2\pm0.1)\times10^{-1}$ (20 °C), $(2.7\pm0.1)\times10^{-1}$ (15 °C), $(2.9\pm0.1)\times10^{-1}$ (10 °C), and $(3.2\pm0.1)\times10^{-1}\,min^{-1}$ (5 °C) (Figure 24b–e). The apparent activation energy $E_a = (-13\pm4)\,kJ\,mol^{-1}$ for the folding of **2** was obtained by Arrhenius plots (Figure 25).

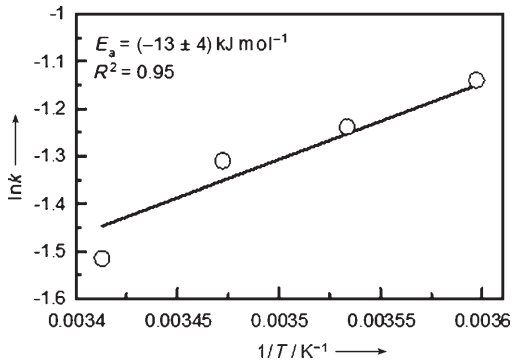

Figure 25. Arrhenius plot for the folding of **2** in toluene.

Acknowledgements

This work was financially supported by the Japan Society for the Promotion of Science (JSPS). H.S. thanks the JSPS for a fellowship for young Japanese scientists. Professor N. Kobayashi and Dr. A. Muranaka (Tohoku University) are also gratefully acknowledged for helpful discussions.

[1] Reviews: diaryl ethenes: a) M. Irie, *Chem. Rev.* **2000**, *100*, 1685–1716; b) H. Tian, S. Yang, *Chem. Soc. Rev.* **2004**, *33*, 85–97; c) Y. Yokoyama, *Chem. Rev.* **2000**, *100*, 1717–1739; spirocyclic compounds, d) G. Berkovic, V. Krongauz, V. Weiss, *Chem. Rev.* **2000**, *100*, 1741–1753; e) V. I. Minkin, *Chem. Rev.* **2004**, *104*, 2751–2776; azo compounds: f) A. Natansohn, P. Rochon, *Chem. Rev.* **2002**, *102*, 4139–4175; g) S. Kawata, Y. Kawata, *Chem. Rev.* **2000**, *100*, 1777–1788; h) B. L. Feringa, *Acc. Chem. Res.* **2001**, *34*, 504–513; i) E. Hadjoudis, I. M. Mavridis, *Chem. Soc. Rev.* **2004**, *33*, 579–588; j) F. M. Raymo, M. Tomasulo, *Chem. Soc. Rev.* **2005**, *34*, 327–336.

[2] a) V. Berl, I. Huc, R. G. Khoury, M. J. Krische, J.-M. Lehn, *Nature* **2000**, *407*, 720–723; b) V. Berl, I. Huc, R. G. Khoury, J.-M. Lehn, *Chem. Eur. J.* **2001**, *7*, 2810–2820.

[3] a) J.-M. Lehn, A. Rigault, J. Siegel, J. Harrowfield, B. Chevrier, D. Moras, *Proc. Natl. Acad. Sci. USA* **1987**, *84*, 2565–2569; b) U. Koert, M. M. Harding, J.-M. Lehn, *Nature* **1990**, *346*. 339–342; c) W. Zarges, J. Hall, J.-M. Lehn, *Helv. Chim. Acta.* **1991**, *74*, 1843–1852; d) T. M. Garrett, U. Koert, J.-M. Lehn, *J. Phys. Org. Chem.* **1992**, *5*, 529–532; e) R. Krämer, J.-M. Lehn, A. Marquis-Rigault, *Proc. Natl. Acad. Sci. USA* **1993**, *90*, 5394–5398.

[4] a) M. Barboiu, G. Vaughan, N. Kyritsakas, J.-M. Lehn, *Chem. Eur. J.* **2003**, *9*, 763–769; see also: b) T. W. Bell, H. Jousselin, *Nature* **1994**, *367*. 441–444.

[5] a) H. Goto, H. Katagiri, Y. Furusho, E. Yashima, *J. Am. Chem. Soc.* **2006**, *128*, 7176–7178; b) H. Katagiri, T. Miyagawa, Y. Furusho, E. Yashima, *Angew. Chem.* **2006**, *118*, 1773–1776; *Angew. Chem. Int. Ed.* **2006**, *45*, 1741–1744.

[6] a) Y. Tanaka, H. Katagiri, Y. Furusho, E. Yashima, *Angew. Chem.* **2005**, *117*, 3935–3938; *Angew. Chem. Int. Ed.* **2005**, *44*, 3867–3870; b) Y. Furushio, Y. Tanaka, E. Yashima. *Org. Lett.* **2006**, *8*, 2583–2586; c) M. Ikeda, Y. Tanaka, T. Hasegawa, Y. Furusho, E. Yashima, *J. Am. Chem. Soc.* **2006**, *128*, 6806–6807.

[7] H. Schlaad, T. Krasia, M. Antonietti, *J. Am. Chem. Soc.* **2004**, *126*, 11307–11310.

[8] H.-C. Yang, S.-Y. Lin, H.-C. Yang, C.-L. Lin, L. Tsai, S.-L. Huang, I. W.-P. Chen, C.-H. Chen, B.-Y. Jin, T.-Y. Luh, *Angew. Chem. Int. Ed.* **2006**, *45*, 727–730.

[9] a) C. Zhang, J.-M. Léger, I. Huc, *Angew. Chem.* **2006**, *118*, 4741–4744; *Angew. Chem. Int. Ed.* **2006**, *45*, 4625–4628; b) D. Haldar, H. Jiang, J.-M. Légr, I. Huc, *Angew. Chem.* **2006**, *118*, 5609–5612; *Angew. Chem. Int. Ed.* **2006**, *45*, 5483–5483.

[10] Examples of kinetic studies of DNA and RNA in double-helix formation and unfolding: a) J. G. Wetmur, N. Davidson, *J. Mol. Biol.* **1968**, *31*, 349–370; b) D. Pörschke, M. Eigen, *J. Mol. Biol.* **1971**, *62*, 361–381; c) M. E. Craig, D. M. Crothers, P. Doty, *J. Mol. Biol.* **1971**, *62*, 383–401; d) S. K. Podder, *Eur. J. Biochem.* **1971**, *22*, 467–477; e) D. Pörschke, O. C. Uhlenbeck, F. H. Martin, *Biopolymers* **1973**, *12*, 1313–1335; f) J. Ravetch, J. Gralla, D. M. Crothers, *Nucleic Acids Res.* **1974**, *1*, 109–127; g) K. J. Breslauer, M. Bina-Stein, *Biophys. Chem.* **1977**, *7*, 211–216; h) J. W. Nelson, I. Tinoco, Jr., *Biochemistry* **1982**, *21*, 5289–5295; i) A. P. Williams, C. E. Longfellow, S. M. Freier, R. Kierzek, D. H. Turner, *Biochemistry* **1989**, *28*, 4283–

4291; j) P. Wu, S.-i. Nakano, N. Sugimoto, *Eur. J. Biochem.* **2002**, *269*, 2821–2830.
[11] Kinetic studies on bulge, triple-helix, or quadruplex formation of RNA and DNA: a) M. Kamiya, H. Trigoe, H. Shindo, A. Sarai, *J. Am. Chem. Soc.* **1996**, *118*, 4532–4538; b) T. Ohmichi, H. Nakamuta, K. Yasuda, N. Sugimoto, *J. Am. Chem. Soc.* **2000**, *122*, 11286–11294; c) A. Ansari, S. V. Kuznetsov, Y. Shen, *Proc. Natl. Acad. Sci. USA* **2001**, *98*, 7771–7776; d) Y. Zhao, Z.-y. Kan, Z.-x. Zeng, Y.-h. Hao, H. Chen, Z. Tan, *J. Am. Chem. Soc.* **2004**, *126*, 13255–13264.
[12] D. J. Hill, M. J. Mio, R. B. Prince, T. S. Hunghes, J. S. Moore, *Chem. Rev.* **2001**. *101*, 3893–4011.
[13] A synthetic single-helix-formation process was examined: W. Y. Yang, R. B. Prince, J. Sabelko, J. S. Moore, M. Gruebele, *J. Am. Chem. Soc.* **2000**, *122*, 3248–3249.
[14] A. Marquis-Rigault, A. Dupont-Gervais, A. V. Dorsserlaer, J.-M. Lehn, *Chem. Eur. J.* **1996**, *2*, 1395–1398.
[15] Computational study of pyridinedicarboxamide to form a double helix: A. Acocella, A. Venturini, F. Zerbetto, *J. Am. Chem. Soc.* **2004**, *126*, 2362–2367.
[16] H. Sugiura, Y. Nigorikawa, Y. Saiki, K. Nakamura, M. Yamaguchi, *J. Am. Chem. Soc.* **2004**, *126*, 14858–14864.
[17] H. Sugiura, M. Yamaguchi, *Chem. Lett.* **2007**, *36*, 58–59.
[18] Y. Saiki, K. Nakamura, Y. Nigorikawa, M. Yamaguchi, *Angew. Chem.* **2003**, *115*, 5348–5350; *Angew. Chem. Int. Ed.* **2003**, *42*, 5190–5192.
[19] a) M. Durand, K. Chevrie, M. Chassignol, N. T. Thuong, J. C. Maurizot, *Nucleic Acids Res.* **1990**, *18*, 6353–6359; b) S. Rumney IV, E. T. Kool, *J. Am. Chem. Soc.* **1995**, *117*, 5635–5646.
[20] a) M. Salunkhe, T. Wu, R. L. Letsinger, *J. Am. Chem. Soc.* **1992**, *114*, 8768–8772; b) S. Bevers, T. P. O'Dea, L. W. McLaughlin, *J. Am. Chem. Soc.* **1998**, *120*, 11004–11005; c) F. D. Lewis, X. Liu, Y. Wu, S. E. Miller, M. R. Wasielewski, R. L. Letsinger, R. Sanishvili, A. Joachimiak, V. Tereshko, M. Egli, *J. Am. Chem. Soc.* **1999**, *121*, 9905–9906; d) F. D. Lewis, Y. Wu, X. Liu, *J. Am. Chem. Soc.* **2002**, *124*, 12165–12173.
[21] a) M. Y.-X. Ma, L. S. Reid, S. C. Climie, W. C. Lin, R. Kuperman, M. Summer-Smith, R. W. Barnett, *Biochemistry* **1993**, *32*, 1751–1758; b) W. Pils, R. Micura, *Nucleic Acids Res.* **2000**, *28*, 1859–1863.
[22] K. Nakamura, H. Okubo, M. Yamaguchi, *Org. Lett.* **2001**, *3*, 1097–1099.
[23] See Supporting Information.
[24] Negative activation energy in the reactions of low-molecular-weight compounds: a) R. Bianchini, C. Chiappe, G. L. Moro, D. Lenoir, P. Lemmen, N. Goldberg, *Chem. Eur. J.* **1999**, *5*, 1570–1580; b) L. P. Olson, K. T. Kuwata, M. D. Bartberger, K. N. Houk, *J. Am. Chem. Soc.* **2002**, *124*, 9469–9475; c) E. A. Mader, A. S. Larsen, J. M. Mayer, *J. Am. Chem. Soc.* **2004**, *126*, 8066–8067; d) K. Ohkubo, S. Fukuzumi, *J. Phys. Chem. A* **2005**, *109*, 1105–1113.
[25] H. Mazaki, T. Watanabe, *Biochim. Biophys. Acta Bioenerg.* **1990**, *1016*, 190–196.
[26] a) D. W. Griffiths, C. D. Gutsche, *J. Am. Chem. Soc.* **1971**, *93*, 4788–4794; b) C. Zioudrou, C. I. Stassinopoulou, S. Loukas, *Bioorg. Chem.* **1980**, *9*, 163–175.
[27] E. Rochlin, Z. Rappoport, *J. Org. Chem.* **2003**, *68*, 1715–1720.

Received: September 13, 2007
Published online: January 18, 2008

